

OFFICE OF CIVILIAN RADIOACTIVE WASTE MANAGEMENT
ANALYSIS/MODEL COVER SHEET
Complete Only Applicable Items

1. QA: QA
 Page: 1 of 55

<p>2. <input checked="" type="checkbox"/> Analysis Check all that apply</p> <table border="1" style="width:100%; border-collapse: collapse;"> <tr> <td style="width:15%;">Type of Analysis</td> <td style="width:10%;">of</td> <td style="width:15%;"><input type="checkbox"/> Engineering</td> <td style="width:60%;"></td> </tr> <tr> <td></td> <td></td> <td><input type="checkbox"/> Performance Assessment</td> <td></td> </tr> <tr> <td></td> <td></td> <td><input checked="" type="checkbox"/> Scientific</td> <td></td> </tr> </table> <table border="1" style="width:100%; border-collapse: collapse;"> <tr> <td style="width:15%;">Intended Use of Analysis</td> <td style="width:10%;">of</td> <td style="width:15%;"><input type="checkbox"/> Input to Calculation</td> <td style="width:60%;"></td> </tr> <tr> <td></td> <td></td> <td><input checked="" type="checkbox"/> Input to another Analysis or Model</td> <td></td> </tr> <tr> <td></td> <td></td> <td><input type="checkbox"/> Input to Technical Document</td> <td></td> </tr> <tr> <td></td> <td></td> <td><input type="checkbox"/> Input to other Technical Products</td> <td></td> </tr> </table> <p>Describe use: Input to Waste Form PMR</p>	Type of Analysis	of	<input type="checkbox"/> Engineering				<input type="checkbox"/> Performance Assessment				<input checked="" type="checkbox"/> Scientific		Intended Use of Analysis	of	<input type="checkbox"/> Input to Calculation				<input checked="" type="checkbox"/> Input to another Analysis or Model				<input type="checkbox"/> Input to Technical Document				<input type="checkbox"/> Input to other Technical Products		<p>3. <input checked="" type="checkbox"/> Model Check all that apply</p> <table border="1" style="width:100%; border-collapse: collapse;"> <tr> <td style="width:15%;">Type of Model</td> <td style="width:10%;">of</td> <td style="width:15%;"><input type="checkbox"/> Conceptual Model</td> <td style="width:60%;"><input type="checkbox"/> Abstraction Model</td> </tr> <tr> <td></td> <td></td> <td><input checked="" type="checkbox"/> Mathematical Model</td> <td><input type="checkbox"/> System Model</td> </tr> <tr> <td></td> <td></td> <td><input type="checkbox"/> Process Model</td> <td></td> </tr> </table> <table border="1" style="width:100%; border-collapse: collapse;"> <tr> <td style="width:15%;">Intended Use of Model</td> <td style="width:10%;">of</td> <td style="width:15%;"><input type="checkbox"/> Input to Calculation</td> <td style="width:60%;"></td> </tr> <tr> <td></td> <td></td> <td><input checked="" type="checkbox"/> Input to another Model or Analysis</td> <td></td> </tr> <tr> <td></td> <td></td> <td><input type="checkbox"/> Input to Technical Document</td> <td></td> </tr> <tr> <td></td> <td></td> <td><input type="checkbox"/> Input to other Technical Products</td> <td></td> </tr> </table> <p>Describe use: Input to Waste Form PMR</p>	Type of Model	of	<input type="checkbox"/> Conceptual Model	<input type="checkbox"/> Abstraction Model			<input checked="" type="checkbox"/> Mathematical Model	<input type="checkbox"/> System Model			<input type="checkbox"/> Process Model		Intended Use of Model	of	<input type="checkbox"/> Input to Calculation				<input checked="" type="checkbox"/> Input to another Model or Analysis				<input type="checkbox"/> Input to Technical Document				<input type="checkbox"/> Input to other Technical Products	
Type of Analysis	of	<input type="checkbox"/> Engineering																																																							
		<input type="checkbox"/> Performance Assessment																																																							
		<input checked="" type="checkbox"/> Scientific																																																							
Intended Use of Analysis	of	<input type="checkbox"/> Input to Calculation																																																							
		<input checked="" type="checkbox"/> Input to another Analysis or Model																																																							
		<input type="checkbox"/> Input to Technical Document																																																							
		<input type="checkbox"/> Input to other Technical Products																																																							
Type of Model	of	<input type="checkbox"/> Conceptual Model	<input type="checkbox"/> Abstraction Model																																																						
		<input checked="" type="checkbox"/> Mathematical Model	<input type="checkbox"/> System Model																																																						
		<input type="checkbox"/> Process Model																																																							
Intended Use of Model	of	<input type="checkbox"/> Input to Calculation																																																							
		<input checked="" type="checkbox"/> Input to another Model or Analysis																																																							
		<input type="checkbox"/> Input to Technical Document																																																							
		<input type="checkbox"/> Input to other Technical Products																																																							

4. Title:
 Clad Degradation—Local Corrosion of Zirconium and Its Alloys under Repository Conditions

8. Document Identifier (including Rev. No. and Change No., if applicable):
 ANL-EBS-MD-000012 REV 00

8. Total Attachments: 3	7. Attachment Numbers - No. of Pages in Each: I-3, II-4, III-5
----------------------------	---

	Printed Name	Signature	Date
8. Originator	Mike Bale	<i>Michael G. Bale</i>	3/24/00
9. Checker	Thomas Thornton	<i>T A Thornton</i>	3/24/00
10. Lead/Supervisor	Christine Stockman	<i>Christine Stockman</i>	3/24/00
11. Responsible Manager	David Stahl	<i>David Stahl</i>	3/24/00

12. Remarks:

**OFFICE OF CIVILIAN RADIOACTIVE WASTE MANAGEMENT
ANALYSIS/MODEL REVISION RECORD**

Complete Only Applicable Items

1. Page: 2 of 55

2. Analysis or Model Title:

Clad Degradation—Local Corrosion of Zirconium and Its Alloys under Repository Conditions

3. Document Identifier (including Rev. No. and Change No., if applicable):

ANL-EBS-MD-000012 REV 00

4. Revision/Change No.

5. Description of Revision/Change

00

Initial Issue

CONTENTS

	Page
ACRONYMS AND ABBREVIATIONS	7
1. PURPOSE.....	8
2. QUALITY ASSURANCE.....	8
3. COMPUTER SOFTWARE AND MODEL USAGE.....	9
4. INPUTS	9
4.1 DATA AND PARAMETERS.....	9
4.1.1 Immersion Corrosion Tests (50.8 mm x 25.4 mm coupons).....	9
4.1.2 Pitting Corrosion Tests (50.8 mm x 25.4 mm coupons).....	14
4.1.3 Crevice Tests (76.2 mm x 25.4 mm coupons).....	15
4.1.4 U-bend Tests (114.3 mm x 19.1 mm coupons).....	17
4.2 CRITERIA.....	18
4.3 CODES AND STANDARDS	18
5. ASSUMPTIONS.....	19
6. ANALYSIS/MODEL	21
6.1 ZIRCONIUM CORROSION–THEORETICAL CONSIDERATIONS	21
6.1.1 Oxide Formation	21
6.1.2 Temperature	22
6.1.3 pH.....	22
6.1.4 Water and Steam	27
6.1.5 Halides	28
6.1.6 Nitrates.....	29
6.1.7 Silicon Dioxide	29
6.1.8 Sulfur and its Compounds.....	30
6.1.9 Pitting.....	32
6.1.10 Crevice Corrosion.....	34
6.1.11 Stress Corrosion Cracking	36
6.1.12 Surface Condition	37
6.1.13 Alloying Elements	38
6.1.14 Irradiation.....	38
6.2 ZIRCONIUM CORROSION–EXPERIMENTAL DATA.....	39
6.2.1 Uniform Corrosion of Zirconium and its Alloys	39
6.2.2 Accelerated Corrosion of Zirconium and its Alloys.....	40
6.2.2.1 Ferric Chloride	41
6.2.2.2 Halide Reactions–Fluoride-Free Solutions	42
6.2.2.3 Halide Reactions–Fluoride-Containing Solutions.....	43
6.2.2.3.1 Data Analysis	43
6.2.2.3.2 Theoretical Evaluation	45

CONTENTS (Continued)

	Page
6.3 CORROSION CRITERIA AND ASSOCIATED RATES	47
7. CONCLUSIONS	47
8. INPUTS AND REFERENCES.....	50
8.1 DOCUMENTS CITED	50
8.2 CODES, STANDARDS, REGULATIONS, AND PROCEDURES	54
ATTACHMENTS.....	55
ATTACHMENT I - "zirc_corr_rate3.xls" SOFTWARE ROUTINE USED TO DEVELOP EQUATIONS 4 AND 5	I-1
ATTACHMENT II - INDUSTRIAL APPLICATIONS OF ZIRCONIUM AND ITS ALLOYS.....	II-1
II.1 UREA	II-1
II.2 ACETIC ACID.....	II-1
II.3 FORMIC ACID.....	II-1
II.4 PEROXIDE AND OTHER SULFURIC ACID-CONTAINING PROCESSES.....	II-2
II.5 HALIDE-CONTAINING PROCESSES.....	II-3
II.6 NITRIC ACID-CONTAINING PROCESSES	II-3
ATTACHMENT III - ZIRCONIUM-METALLURGY	III-1
III.1 GENERAL	III-1
III.2 ZIRCONIUM CHARACTERISTICS	III-1
III.3 GENERAL CORROSION OF ZIRCONIUM AND ITS ALLOYS	III-3
III.4 ENVIRONMENTAL CONDITIONS–J-13 WELL WATER.....	III-4

FIGURES

	Page
Figure 1a. The Potential-pH Diagram of Zirconium in Water at 25°C	23
Figure 1b. Theoretical Conditions of Corrosion, Immunity, and Passivation of Zirconium at 25°C	24
Figure 2. The Potential-pH Diagram of Iron in Water at 25°C.....	25
Figure 3. The Potential-pH Diagram of Fluorine in Water at 25°C.....	27
Figure 4. The Iso-Corrosion Diagram of Zr 702 in Sulfuric Acid.....	30
Figure 5. The Iso-Corrosion Diagram of Zr 704 in Sulfuric Acid.....	31
Figure 6. The Iso-Corrosion Diagram of Zr 705 in Sulfuric Acid.....	31
Figure 7. The Electrochemical Behaviors of Stainless Steel and Zirconium.....	32
Figure 8. The Corrosion Process within a Pit	34
Figure 9. Crevice Corrosion.....	35
Figure 10. Surface Effect on the Rest Potential of Zr 702 in 10% HCl Plus 500 ppm Ferric Ion at 30°C	38
Figure 11. Predicted versus Measured Corrosion Rate as a Function of pH, F ⁻ , and Cl ⁻	44

TABLES

	Page
Table 1. Corrosion Rates from Experiment with Varying Solutions of Chlorides and Fluorides at 80°C for 12 Hours.....	13
Table 2. Corrosion Rates from Experiment with Varying Solutions of Chlorides and Fluorides at 80°C for 24 Hours.....	13
Table 3. Corrosion Rates from Experiment with Varying Solutions of Chlorides and Fluorides at 55°C for 24 Hours.....	14
Table 4. Corrosion Testing of Abraded Zr 702 Welded Coupons.....	15
Table 5. U-bend Tests of Zr 702 with Varying Test Conditions.....	18
Table 6. Dissolved Fluoride Ions in Mixed Solutions.....	26
Table 7. Reduction/Oxidation Pairs.....	33
Table 8. A Simplified Set of Data Derived from Data in 4.1.1 Tests 10 to 13.....	45
Table III.1 Nuclear and Non-nuclear Grades of Zirconium Alloys.....	III-3
Table III.2. Compositions of J-13 Well Water and Its Concentrates.....	III-5

ACRONYMS AND ABBREVIATIONS

AMR	Analysis Model Report
BAPL	Bettis Atomic Power Laboratory
BWR	boiling water reactor
c.d.	current density
CPI	chemical process industry
CSNF	commercial spent nuclear fuel
LCNW	longitudinal cut nonwelded
LCW	longitudinal cut welded
mpy	mills per year
NHE	normal hydrogen electrode
pH	the negative logarithm of the hydrogen ion activity
PTFE	polytetrafluoroethylene
PWR	pressurized water reactor
SCC	stress corrosion cracking
SCE	standard calomel electrode
SHE	standard hydrogen electrode
SNF	spent nuclear fuel
TCNW	transverse cut non-welded
TCW	transverse cut welded
TSPA	Total System Performance Assessment

1. PURPOSE

The United States Department of Energy (DOE) Office of Civilian Radioactive Waste Management (OCRWM) is assessing the designs of waste packages for storage and disposal of high-level radioactive waste and spent nuclear fuel. Because the majority of the spent nuclear fuel is Zircaloy-clad UO_2 fuel pellets, evaluations are being made to determine whether the Zircaloy cladding could be considered as a major component of the containment system. An essential part of this Analysis Model Report (AMR) is an estimate of the corrosion rate of Zircaloy cladding under typical and atypical conditions.

The primary purpose of this AMR is to assess the conditions under which zirconium and its alloys might suffer accelerated or enhanced corrosion. Available data from nuclear and non-nuclear corrosion tests have been reviewed and, where possible, accelerated corrosion data have been analyzed to provide a correlation between the corrosion rates and the halide content of the environment. The review includes discussion of high general corrosion, pitting, crevice corrosion, and stress corrosion cracking (SCC). General information on the history, processing, and uses of zirconium is included in an attachment to emphasize the unique position of zirconium in nuclear and chemical process industry (CPI) applications.

It should be noted that although Zircaloy-2 and Zircaloy-4 have both been extensively studied for their corrosion and oxidation properties in nuclear power plants, few studies have been performed on the corrosion resistance of either alloy under the aggressive corrosion conditions addressed in this AMR, particularly in environments with high halide concentrations.

This AMR was developed in accordance with this development plan, *Waste Package Materials Department Analysis and Modeling Reports Supporting the Waste Form PMR* (CRWMS M&O 2000a). The scope of this AMR is outlined in “Clad Degradation—Local Corrosion of Zirconium and Its Alloys under Repository Conditions” of the development plan.

2. QUALITY ASSURANCE

The Quality Assurance (QA) program applies to this analysis. All types of waste packages were classified (per QAP-2-3) as Quality Level-1 in *Classification of the MGR Uncanistered Spent Nuclear Fuel Disposal Container System* (CRWMS M&O 1999a, p. 7). This analysis applies to all of the waste package designs included in the MGR classification Analyses. Reference CRWMS M&O (1999a) is cited as an example. The development of this analysis is conducted under the *Activity Evaluation for 1101213FM3 Waste Form Analyses & Models—PMR* (CRWMS M&O 1999b), which was prepared per QAP-2-0. The results of that evaluation were that the activity is subject to the *Quality Assurance Requirements and Description* (DOE 2000) requirements.

3. COMPUTER SOFTWARE AND MODEL USAGE

One software routine was used in the preparation of the equations in Section 6.2 of this AMR (zirc corr rate3.xls, Version 1); this routine is documented by a complete listing in Attachment I. The routine was developed under Microsoft Excel 97 SR-2, an exempt software, which in turn was running under Microsoft Windows 95. The routine has been verified for positive values in cells B3..C26 and nonnegative values in cells D3..J26, provided that the total fluoride and chloride concentrations are positive. Error conditions noted by “#NUM!” in rows 9, 13, and 17 result from zero fluoride concentrations and a zero corrosion rate. The results of these rows were not included in further calculations and are included only for completeness. The correctness of the results has been verified by hand calculations.

The model for the uniform corrosion rate of Zircaloy-2 and Zircaloy-4 that is recommended in this AMR is that derived by Hillner, Franklin, and Smee working under contract DE-AC11-93PN38195 at Bettis Atomic Power Laboratory (BAPL). The report title is *The Corrosion of Zircaloy-Clad Fuel Assemblies in a Geologic Repository Environment*. The model and equation constants obtained by Hillner et al. (1998) are similar to models developed by others as noted in the BAPL report.

4. INPUTS

Yau and Webster (1987, pp. 711-715) originally published the following data in a summarized form. It provides the corrosion results obtained during the 1980s and 1990s at Wah Chang. For the current report, the original data were re-examined and the actual results are provided below, together with statistical analysis where possible. Since zirconium and zirconium alloy corrosion tests can result in weight losses or gains depending on conditions, all data reported below shall be considered as weight losses except where otherwise noted in the text and where results are indicated with a + sign. It should be stressed that although the corrosion rates are quoted in micron per year or mm per year, the actual tests were of relatively short duration, and the predicted annual rates can decrease (or increase) as the experimental time increases. This effect is illustrated by the data given in Section 4.1.2.

4.1 DATA AND PARAMETERS

4.1.1 Immersion Corrosion Tests (50.8 mm x 25.4 mm coupons).

Test 1—Conditions and durations: NaCl (25%) (pH = 1) at boiling for 504 hours.

Results: No pitting.

Observed corrosion rates:

Zr 702	0.66 $\mu\text{m}/\text{yr}$, 0.38 $\mu\text{m}/\text{yr}$ Mean value, 0.52 $\mu\text{m}/\text{yr}$ σ (standard deviation), 0.14 $\mu\text{m}/\text{yr}$
Zr 705	0.18 $\mu\text{m}/\text{yr}$, 0.0 $\mu\text{m}/\text{yr}$ Mean value, 0.09 $\mu\text{m}/\text{yr}$ σ , 0.09 $\mu\text{m}/\text{yr}$

Test 2—Conditions and durations: FeCl₃ solutions at ambient temperature for 192 hours.

Results: Pitting.

Observed corrosion rates:

Non-welded Zr 702 in 10% FeCl ₃ at 25°C	230 μm/yr
Welded Zr 702 in 10% FeCl ₃ at 25°C	> 1,270 μm/yr
Non-welded Zr 702 in 6% FeCl ₃ at 50°C	48 μm/yr

Test 3—Conditions and durations: FeCl₃ (10%) at boiling for 96 hours.

Observed corrosion rates for non-welded Zr 702:

As-received	533 μm/yr
1-minute pickled	9.9 μm/yr
2-minute pickled	1.5 μm/yr
3-minute pickled	0.0 μm/yr
4-minute pickled	0.0 μm/yr

Observed corrosion rates for welded Zr 702:

As-welded	> 5,000 μm/yr
1-minute pickled	71 μm/yr
2-minute pickled	41 μm/yr
3-minute pickled	7.9 μm/yr
4-minute pickled	4.3 μm/yr

*Note: Pickling involves immersion of the cladding in a weak acid. See Section 6.1.12 for discussion of pickling

Test 4—Conditions and durations: NaCl (5%) + CH₃COOH (0.5%) + saturated H₂S at 100°C for 283 hours (a simulation of certain underground fluids such as geothermal fluids).

Corrosion rates in the liquid phase: All coupons showed **weight gains**.

Zr 702	+ 1.70 μm/yr, + 2.63 μm/yr
	Mean value, + 2.165 μm/yr
	σ, 0.465 μm/yr
Zr 705	+ 3.33 μm/yr, + 3.33 μm/yr
	Mean value, + 3.33 μm/yr
	σ, 0.0 μm/yr

Corrosion rates in the vapor phase: All coupons showed **weight gains or no change**.

Zr 702	0.0 μm/yr, 0.0 μm/yr
--------	----------------------

Mean value, 0.0 $\mu\text{m}/\text{yr}$
 σ , 0.0 $\mu\text{m}/\text{yr}$

Zr 705 + 0.56 $\mu\text{m}/\text{yr}$, + 0.56 $\mu\text{m}/\text{yr}$
Mean value, + 0.56 $\mu\text{m}/\text{yr}$
 σ , 0.0 $\mu\text{m}/\text{yr}$

Test 5—Conditions and durations: NaCl (25%), CH₃COOH (0.5%), S (0.1%), saturated H₂S at 250°C in an autoclave under pressure for 1,824 hours (a simulation of certain underground fluids such as geothermal fluids).

Corrosion rates: All coupons showed **weight gains**.

Non-welded Zr 702	+ 0.15 $\mu\text{m}/\text{yr}$
Welded Zr 702	+ 0.41 $\mu\text{m}/\text{yr}$
Non-welded Zircaloy-4	+ 0.48 $\mu\text{m}/\text{yr}$
Welded Zircaloy-4	+ 0.36 $\mu\text{m}/\text{yr}$
Non-welded Zr 705	+ 0.18 $\mu\text{m}/\text{yr}$
Welded Zr 702	+ 0.46 $\mu\text{m}/\text{yr}$

Test 6—Conditions and durations: Seawater at boiling for 275 days.

Corrosion rates: All coupons showed **weight gains**.

Non-welded Zr 702	+ 0.13 $\mu\text{m}/\text{yr}$, + 0.12 $\mu\text{m}/\text{yr}$ Mean value, + 0.125 $\mu\text{m}/\text{yr}$ σ , 0.005 $\mu\text{m}/\text{yr}$
Welded Zr 702	+ 0.14 $\mu\text{m}/\text{yr}$, + 0.12 $\mu\text{m}/\text{yr}$ Mean value, + 0.13 $\mu\text{m}/\text{yr}$ σ , 0.01 $\mu\text{m}/\text{yr}$
Non-welded Zr 705	+ 0.14 $\mu\text{m}/\text{yr}$, + 0.19 $\mu\text{m}/\text{yr}$ Mean value, + 0.165 $\mu\text{m}/\text{yr}$ σ , 0.025 $\mu\text{m}/\text{yr}$
Welded Zr 705	+ 0.18 $\mu\text{m}/\text{yr}$, + 0.22 $\mu\text{m}/\text{yr}$ Mean value, + 0.20 $\mu\text{m}/\text{yr}$ σ , 0.02 $\mu\text{m}/\text{yr}$

Test 7—Conditions and durations: Seawater at 200°C in an autoclave under pressure for 1480 hours.

Corrosion rates: All coupons showed **weight gains**.

Zr 702	+ 0.76 $\mu\text{m}/\text{yr}$
Zircaloy-2	+ 2.29 $\mu\text{m}/\text{yr}$
Zr 705	+ 1.02 $\mu\text{m}/\text{yr}$

Test 8—Conditions and durations: Concentrated seawater at 149°C for 60 days (seawater was concentrated by boiling off 400 ml from 1000 ml seawater).

Corrosion rates: All coupons showed **weight gains**.

Non-welded Zr 702	+ 0.10 $\mu\text{m}/\text{yr}$ in liquid, + 0.03 $\mu\text{m}/\text{yr}$ in vapor
Welded Zr 702	+ 0.17 $\mu\text{m}/\text{yr}$ in liquid, + 0.067 $\mu\text{m}/\text{yr}$ in vapor

Test 9—Conditions and durations: HCl (10%) + 3,450 ppm Fe^{3+} (1% FeCl_3) for 6 days (abraded Zr 702 cylindrical specimens with 600 grit SiC paper for these tests).

Corrosion rates: 1,300; 4,300; and 4,600 $\mu\text{m}/\text{yr}$ at 65; 90; and 102°C, respectively.

Test 10—Conditions and durations: City water (pH = 7) + 100 ppm F^- at 100°C for 24 hours (city water is fluoridated with 1 ppm F^- as sodium fluorosilicate).

Corrosion rates for experiment with F^- added as NaF:

Zr 702	7.87 $\mu\text{m}/\text{yr}$, 3.81 $\mu\text{m}/\text{yr}$
	Mean value, 5.84 $\mu\text{m}/\text{yr}$
	σ , 2.03 $\mu\text{m}/\text{yr}$

Corrosion rates with F^- added as sodium monofluorophosphate in toothpaste:

Zr 702	7.87 $\mu\text{m}/\text{yr}$, 7.87 $\mu\text{m}/\text{yr}$
	Mean value, 7.87 $\mu\text{m}/\text{yr}$
	σ , 0.0 $\mu\text{m}/\text{yr}$

Note: Tests 10 and 11 conducted in virgin polytetrafluoroethylene (PTFE) vessels (see text).

Test 11—Conditions and durations: HCl (10%) + HF at 30°C for 72 hours.

Corrosion rates from experiment with HF in solution at a concentration of 5 ppm:

Zr 702	76.2 $\mu\text{m}/\text{yr}$, 76.2 $\mu\text{m}/\text{yr}$
	Mean value, 76.2 $\mu\text{m}/\text{yr}$
	σ , 0.0 $\mu\text{m}/\text{yr}$

Corrosion rates from experiment with HF in solution at a concentration of 20 ppm:

Zr 702 102 $\mu\text{m}/\text{yr}$, 127 $\mu\text{m}/\text{yr}$
 Mean value, 114.5 $\mu\text{m}/\text{yr}$
 σ , 12.5 $\mu\text{m}/\text{yr}$

Test 12–Conditions and durations: Chlorides and Fluorides (Mixed Solutions) at 80°C

Table 1. Corrosion Rates from Experiment with Varying Solutions of Chlorides and Fluorides at 80°C for 12 Hours

CaCl ₂ (%)	MgCl ₂ (%)	F as NaF (ppm)	F as CaF ₂ (ppm)	pH	Corrosion rate (mm/yr)
0.2	0.1	5	0	1	0.03
0.2	0.1	20	0	1	0.43
2.0	1.0	5	0	1	0.02
2.0	1.0	20	0	1	0.21
6.6	3.3	5	0	1	0.01
6.6	3.3	20	0	1	0.24

NOTE: Test 12 conducted in virgin PTFE vessels (see text).

Table 2. Corrosion Rates from Experiment with Varying Solutions of Chlorides and Fluorides at 80°C for 24 Hours

CaCl ₂ (%)	MgCl ₂ (%)	F as NaF (ppm)	F as CaF ₂ (ppm)	pH	Corrosion rate (mm/yr)
0.2	0.1	0	0	1	0.01
0.2	0.1	200	100	1	8.79
0.2	0.1	0	300	1	8.79
0.2	0.1	200	100	3	0.17
2.0	1.0	0	0	1	0.0
2.0	1.0	200	2800	1	2.87
2.0	1.0	0	300	1	3.71
2.0	1.0	200	2800	3	0.01
6.6	3.3	0	0	1	0.01
6.6	3.3	200	9800	1	1.92
6.6	3.3	0	300	1	1.02
6.6	3.3	200	9800	3	0.01

NOTE: Test 13 conducted in virgin PTFE vessels (see text).

Test 13–Conditions and durations: Chlorides and fluorides (mixed solutions) at 55°C for 24 hours.

Table 3. Corrosion Rates from Experiment with Varying Solutions of Chlorides and Fluorides at 55°C for 24 Hours

CaCl ₂ (%)	NaCl (%)	MgCl ₂ (%)	KCl (%)	F ⁻ as NaF (ppm)	F ⁻ as CaF ₂ (ppm)	pH	Corrosion rate (mm/yr)
1.5	1.5	1.0	1.0	5000	0	1	16.3
1.5	1.5	1.0	1.0	5000	0	5	0.008
1.5	1.5	1.0	1.0	1000	4000	5	0.006
1.5	1.5	1.0	1.0	1000	4000	1	10.6
1.5	1.5	1.0	1.0	1000	0	6.5	0.006
1.5	1.5	1.0	1.0	1000	0	1	9.40

NOTE: Experiment conducted in virgin PTFE vessels (see text)

4.1.2 Pitting Corrosion Tests (50.8 mm x 25.4 mm coupons)

A set of Zr 702 welded coupons was immersed in the test solutions. The coupons were abraded with 600 grit SiC paper to enhance the pitting susceptibility. Separate coupons were removed from each test solution at days 8, 32, and 64. The depth of the pit was measured in one of two ways. A microscope was focused on the surface of the specimen and then on the bottom of the pit. The movement of the microscope was taken as the pit depth. Alternately, the thickness of the sample was measured, and the surface was then ground until all pits were removed. The sample thickness was remeasured, and the difference in thickness values was taken as the pit depth. The 10 wt.% and 20 wt.% HCl solutions were not changed during the test period. Instead, a constant solution volume was maintained daily by adding either distilled water or freshly prepared 20% HCl to the 10% and 20% HCl, respectively. The 37% HCl solutions were changed once a week.

Table 4. Corrosion Testing of Abraded Zr 702 Welded Coupons

HCl (wt%)	Temp. (°C)	Fe ³⁺ (ppm)	8 days (µm/yr ^a)	32 days (µm/yr ^a)	64 days (µm/yr ^a)
10	30	50	0.0/0.0/0.0	0.0/0.0/0.0	0.0/0.0/0.0
		100	2.0/0.0/0.0	0.3/0.0/0.0	0.3/0.0/0.0
		500	5.1/0.0/0.0	2.3/0.0/0.0	2.0/0.0/0.0
	60	50	0.0/0.0/0.0	0.3/0.0/0.0	0.0/0.0/0.0
		100	2.5/0.0/0.0	1.0/0.0/0.0	0.3/0.0/0.0
		500	8.1/0.0/0.0	4.6/180/360	4.1/460/180
	85	50	0.0/0.0/0.0	0.5/0.0/0.0	0.3/46/0.0
		100	2.8/0.0/0.0	0.8/91/0.0	0.5/61/0.0
		500	11.4/360/480	6.1/1200/1300	4.8/61/1200
	102	50	0.3/0.0/0.0	0.3/0.0/0.0	0.3/180/170
		100	3.6/0.0/0.0	0.5/180/210	0.5/120/91
		500	9.1/480/680	5.1/1300/1200	5.6/480/350
20	30	50	0.0/0.0/0.0	0.0/0.0/0.0	0.0/0.0/0.0
		100	1.3/0.0/0.0	1.0/0.0/0.0	0.5/0.0/0.0
		500	7.9/0.0/0.0	6.6/0.0/0.0	6.1/110/180
	60	50	0.0/0.0/0.0	0.5/0.0/0.0	0.1/0.0/0.0
		100	2.5/0.0/0.0	1.0/0.0/0.0	2.5/61/0.0
		500	1.6/0.0/0.0	7.6/91/360	4.8/86/250
	85	50	2.8/0.0/0.0	3.6/0.0/0.0	6.1/46/0.0
		100	5.1/0.0/0.0	2.0/0.0/0.0	5.8/0.0/0.0
		500	12/800/910	6.1/740/2600	13/200/1200
	107	50	13/0.0/0.0	7.1/0.0/0.0	13/51/30
		100	33/0.0/0.0	25/0.0/0.0	19/0.0/0.0
		500	9.1/1100/680	6.1/740/2600	2.8/3600/5200
37	30	50	94/0.0/0.0	66/0.0/0.0	86/0.0/0.0
		100	46/0.0/0.0	18/0.0/0.0	19/0.0/0.0
		500	41/0.0/0.0	48/0.0/0.0	48/0.0/0.0
	53	50	61/0.0/0.0	81/0.0/0.0	150/0.0/0.0
		100	28/0.0/0.0	84/0.0/0.0	130/0.0/0.0
		500	19/0.0/0.0	69/0.0/0.0	100/0.0/0.0

NOTE: ^a General corrosion rate/maximum pitting rate in the parent metal/maximum pitting rate in the weld metal

4.1.3 Crevice Tests (76.2 mm x 25.4 mm coupons).

Test 1—Conditions and durations: NaCl (25%) + 50 ppm Fe³⁺ (pH = 1) at boiling for seven 1-day runs

Results: No pitting or crevice corrosion.

General corrosion rates:

Zr 702 + 0.10 µm/yr, + 0.10 µm/yr (**weight gains**)

Mean value, + 0.10 µm/yr

σ, 0.0 µm/yr

Zr 705 8.40 µm/yr, 12.4 µm/yr

Mean value, 10.4 µm/yr

σ, 2.0 µm/yr

Test 2—Conditions and durations: NaCl (25%) + 100 ppm Fe³⁺ (pH = 1) at boiling for seven 1-day runs

Results: No pitting or crevice corrosion.

General corrosion rates:

Zr 702	+ 0.84 $\mu\text{m}/\text{yr}$, + 1.00 $\mu\text{m}/\text{yr}$ (weight gains) Mean value, + 0.92 $\mu\text{m}/\text{yr}$ σ , 0.08 $\mu\text{m}/\text{yr}$
Zr 705	25.2 $\mu\text{m}/\text{yr}$, 19.6 $\mu\text{m}/\text{yr}$ Mean value, 22.4 $\mu\text{m}/\text{yr}$ σ , 2.8 $\mu\text{m}/\text{yr}$

Test 3—Conditions and durations: NaCl (25%) + 200 ppm Fe³⁺ (pH = 1) at boiling for seven 1-day runs

Results: No pitting or crevice corrosion.

General corrosion rates:

Non-welded Zr 702	+ 0.10 $\mu\text{m}/\text{yr}$, + 0.10 $\mu\text{m}/\text{yr}$ (weight gains) Mean value, + 0.10 $\mu\text{m}/\text{yr}$ σ , 0.0 $\mu\text{m}/\text{yr}$
Welded Zr 702	216 $\mu\text{m}/\text{yr}$, 224 $\mu\text{m}/\text{yr}$ Mean value, 220 $\mu\text{m}/\text{yr}$ σ , 4 $\mu\text{m}/\text{yr}$
Non-welded Zr 705	36.8 $\mu\text{m}/\text{yr}$, 31.0 $\mu\text{m}/\text{yr}$ Mean value, 33.9 $\mu\text{m}/\text{yr}$ σ , 2.9 $\mu\text{m}/\text{yr}$

Test 4—Conditions and durations: NaCl (25%) + 50 ppm Fe³⁺ (pH = 3) at boiling for seven 1-day runs.

Results: No pitting or crevice corrosion

General corrosion rates:

Zr 702	+ 7.42 $\mu\text{m}/\text{yr}$, + 8.30 $\mu\text{m}/\text{yr}$ (weight gains) Mean value, + 7.86 $\mu\text{m}/\text{yr}$ σ , 0.44 $\mu\text{m}/\text{yr}$
Zr 705	3.80 $\mu\text{m}/\text{yr}$, 4.32 $\mu\text{m}/\text{yr}$ Mean value, 4.06 $\mu\text{m}/\text{yr}$ σ , 0.26 $\mu\text{m}/\text{yr}$

Test 5—Conditions and durations: NaCl (25%) + 100 ppm Fe³⁺ (pH = 3) at boiling for seven 1-day runs.

Results: No pitting or crevice corrosion.

General corrosion rates:

Zr 702 + 6.19 μm/yr, + 5.73 μm/yr (**weight gains**)
Mean value, + 5.96 μm/yr
σ, 0.23 μm/yr

Zr 705 4.32 μm/yr, 5.08 μm/yr
Mean value, 4.70 μm/yr
σ, 0.38 μm/yr

Test 6—Conditions and durations: NaCl (25%) + 200 ppm Fe³⁺ (pH = 3) at boiling for seven 1-day runs.

Results: No pitting or crevice corrosion.

General corrosion rates:

Zr 702 + 5.28 μm/yr, + 4.50 μm/yr (**weight gains**)
Mean value, + 4.89 μm/yr
σ, 0.39 μm/yr

Zr 705 + 6.60 μm/yr, + 3.56 μm/yr (**weight gains**)
Mean value, + 5.08 μm/yr
σ, 1.53 μm/yr

Test 7—Conditions and durations: NaCl (saturated) (pH = 0) at boiling for 306 hours.

Results: No pitting or crevice corrosion.

General corrosion rates:

Zr 702 + 4.20 μm/yr (**weight gain**)
Zircaloy-2 2.54 μm/yr

4.1.4 U-bend Tests (114.3 mm x 19.1 mm coupons)

U-bend test samples were prepared as a function of the rolling direction: longitudinal cut non-welded (LCNW), transverse cut nonwelded (TCNW), longitudinal cut welded (LCW) and transverse cut welded (TCW). The weld was a longitudinal weld. Although Zr 702 bolts and nuts were used in most cases, steel bolts and nuts were used in some instances in an effort to induce galvanic reaction.

Test 1–Seawater and chloride solutions.

U-bend tests of Zr 702 and Zircaloy-2, with and without steel coupling, were performed under the following conditions. No cracking was observed in the zirconium alloys although the steel bolts and nuts corroded badly during the test.

1. Seawater at boiling (101°C) for 365 days.
It was noted that the **welded** Zircaloy-2 U-bend sample became embrittled due to the high absorption of hydrogen (450 ppm) and oxygen (3,500 ppm).
2. NaCl (20%) at boiling (107°C) for 60 days.
3. NaCl (5%) + CH₃COOH (0.5%) + Saturated H₂S at boiling (102°C) for 60 days.
(This was intended as a simulation of certain underground fluids such as geothermal fluids.)

Test 2–HCl solutions

U-bend tests of Zr 702 using Zr 702 bolts and nuts were performed under the conditions shown in [Table 5](#).

Table 5. U-bend Tests of Zr 702 with Varying Test Conditions

Solution	Temperature (°C)	Time to Failure (days)			
		TCNW	LCNW	TCW	LCW
10% HCl + 100 ppm Fe ³⁺	30	6	5
	100	(30) ^a	(30) ^a
20% HCl + 100 ppm Fe ³⁺	30	(30) ^a	(30) ^a
	100	(30) ^a	2
10% HCl + 500 ppm Fe ³⁺	30	5; 7	5; 7	7	1
	60	1; 7	6; 8	0.1	0.1
	85	14	(30) [†]	0.1	0.1
	100	(30) ^a	(30) [†]	0.1	0.1; 0.5
20% HCl + 500 ppm Fe ³⁺	30	(30) ^a	(30) [†]	(30) [†]	(30) ^a
	60	(30) ^a	(30) [†]	(30) [†]	6
	85	(30) ^a	(30) [†]	0.1	0.1
	100	(30) ^a	(30) [†]	0.1	0.1; 0.5

NOTE: ^a No cracking was observed after 30 days of test.

4.2 CRITERIA

There are no criteria that are directly applicable to the analysis or model subject. However, equations similar to those given for the uniform corrosion rate model are used to calculate the cladding oxide growth obtained during in-reactor irradiation and to assure that the resulting oxide layer does not exceed the licensed thickness limits agreed upon between the Nuclear Regulatory Commission and fuel vendors.

4.3 CODES AND STANDARDS

No codes or standards were used in the derivation of the relationships given in the text.

5. ASSUMPTIONS

The following assumptions have been made to enable the analyses and model development in this report:

- It is assumed that variations in hafnium content have negligible impact on the corrosion rate of zirconium and its alloys provided other chemical and processing conditions are maintained constant. The rationale for this assumption is that hafnium is "without effect in the range 0-2.0%" (Lustman and Kerze 1955, Table 11.27, p.631 and p. 618) that hafnium is innocuous at the usual impurity level. Zirconium and its alloys are generally classified into two categories, nuclear and non-nuclear. The main difference between the nuclear and non-nuclear grades is the hafnium content (see Attachment III, Table III.1). Nuclear grades have less than 100 ppm; whereas, the non-nuclear grades may contain up to 4.5% of the element. Hafnium has a high neutron cross section and, therefore, a major impact on the nuclear properties of zirconium, but its effect on the mechanical and chemical properties of zirconium and its alloys is negligible. Thus the corrosion data obtained on non-nuclear and nuclear grades of the element and its alloys materials are considered equivalent. The assumption that hafnium levels within the limits allowed for commercial spent nuclear fuel (CSNF) cladding does not materially affect corrosion rates is used in Section 6.2 of this report to derive a common corrosion model for all the commercial fuel cladding alloys under repository conditions. This assumption does not require validation because the negligible impact of hafnium content within the limits required for Zircaloy cladding validated by means of technical review through publication in the open literature and because the data treatment in this AMR develops/abstracts conservative models, which bound all hafnium compositions.
- It is assumed that the alloy compositions of the non-nuclear grade Zr 704 (R60704) and the nuclear grades Zircaloy-2 (R60802) and Zircaloy-4 (60804) are sufficiently close to each other that the corrosion characteristics of all three alloys are comparable. The rationale for this assumption is the fact that all commercial fuel cladding compositions have low alloy contents and are based on the low-temperature alpha structure with dilute additions of either solid solution strengthening or alpha stabilizing elements such as oxygen and tin. Some information concerning the corrosion behavior of non-nuclear grades are given in Attachment III in further support of the assumption. The corrosion behavior of the several grades and specifications of zirconium alloy used for fuel cladding in commercial light water reactors can be represented by conservative models, which bound all the grades. That is, separate localized corrosion models for the various grades of CSNF cladding are not required for the TSPA. This assumption is used throughout this report. This assumption is partially validated by the accepted engineering practice within the commercial nuclear fuel industry of assuring that the composition of zirconium alloys used for cladding conforms to the ASTM requirements for these nuclear-grade alloys. Further validation of this assumption is not required because the compositions of the CSNF cladding are within the limits set for the nuclear grade alloys and because data treatment in this AMR develops/abstracts conservative models which bound all grades.
- It is assumed in this AMR that the repository environment to which the CSNF cladding could be exposed does not include certain very aggressive chemical conditions, and that

the cladding will generally oxidize at a linear post-transition (from a black to a gray oxide coating) rate that is significantly less than the pre-transition rate observed in the early stages of Zircaloy corrosion. The chemical environments not considered are those containing copper chlorides and certain organic compounds, which are not considered to be present in the waste package. This assumption is used in this AMR to justify the form of the corrosion model developed in Section 6.2. The assumption that the cladding will not be exposed to very aggressive chemical environments has been validated by CRWMS M&O (2000b), the in-package chemistry AMR. The assumption that the cladding will oxidize at the post-transition rate does not require validation since this is widely accepted in the open literature (for example, Yau and Webster 1987; Jangg et al. 1978; Hillner et al. 1998; Etherington et al. 1955; Cheng et al. 1994) on zirconium alloy corrosion and thus is validated by means of technical review through publication in the open literature. This assumption is used throughout the analyses in Section 6. The results and conclusions of this report may significantly overpredict uniform corrosion rates since worst case data has been selected from the literature (Hillner et al. 1998).

- It is assumed in this AMR that the corrosion rate of Zircaloy in highly concentrated J-13 well water may be represented for the purposes of localized corrosion modeling by the corrosion rate in the J-13 solution composition, a fluoride-containing concentrated solution similar to that given in [Table III.2](#) of Attachment III and the corrosion rate in a similar concentrated solution but without the fluoride. The expected temperature is around 100°C, and the solution pH will be higher than 3.18 as well ([See Figure 3](#)). The rationale for this assumption is supported by the discussion above and partially validated by the general acceptance in the open literature concerning the effect of fluorides on zirconium alloy corrosion. This assumption will be used to justify application of the corrosion models to the repository TSPA condition in Section 6.2. This assumption is further validated by the results of CRWMS M&O (2000b), the in-package chemistry AMR.

6. ANALYSIS/MODEL

6.1 ZIRCONIUM CORROSION–THEORETICAL CONSIDERATIONS

6.1.1 Oxide Formation

In many respects, zirconium behaves like other passive metals such as titanium, iron, nickel, and chromium. All rely on the formation of a passive-oxide film for corrosion resistance. However, zirconium is unique in the following respects.

1. As shown by Whitton (1968, p. 60), the growth rate of the zirconium oxide film is controlled by the migration of oxygen (O^{2-}) ions through the existing oxide film. Oxide growth continues at the metal/oxide interface. The initial oxide layer forms spontaneously; however, additional oxide layers form at much reduced and decreasing rates as a result of the initial oxide layer. This mechanism provides zirconium with a self-healing capability when surface damage occurs provided the damage occurs in an oxygen-containing environment.
2. The composition of the zirconium oxide is invariably considered to be ZrO_2 . Compared to the passive films formed on other elements, which may be of variable valency states, Pourbaix (1966, p. 228) suggests that zirconium exists only with the valency of four. This single valency state is also proposed by Shunk (1969, p. 590) although he does reference the possibility of a lower valence sub-oxide when very thin films are considered.
3. The electrical behavior of ZrO_2 is closer to that of an insulator than a semiconductor. The chemical bonding between zirconium and oxygen is very strong at 6.6 eV per equivalent. The current transport passing through the film becomes increasingly difficult as the film grows. It can proceed at areas like grain boundaries and atomic-defect sites. Due to this behavior, it is questioned whether realistic corrosion rates can be obtained from electrochemical studies, since measurements can only be made when the oxide layer is relatively thin and not typical of irradiated cladding conditions.

Although the oxide has the single composition ZrO_2 as noted in #2 above, it may exist in three crystallographic forms: cubic, tetragonal, and monoclinic. Burgers et al. (1932, pp. 599-600) reported the oxide film on zirconium during anodic polarization in a phosphoric solution to be monoclinic; whereas, Charlesby (1953, p. 346) observed a cubic structure for the anodic film produced during polarization in 0.1N HNO_3 . By contrast Cox (1970, p. 658) noted that the film formed in 1N HNO_3 was unique, being essentially all monoclinic; whereas, all other oxide films formed in the experiments had a large percentage of the cubic phase with only traces of the monoclinic structure. In all cases, the oxide film was very thin. Additional discussion on crystallographic forms is available in Shunk (1969, p. 590).

When a thick oxide is produced on cladding from reaction with steam or water, most of the oxide exists as the monoclinic structure. However, the tetragonal structure appears to be retained when a thin oxide is formed under high compressive stresses, for example, the adherent film immediately adjacent to the metal surface. Roy and David (1970, p. 78)

observed this condition during Zircaloy-2 investigations. Similarly, Godlewski et al. (1991, pp. 423, 433) and Godlewski (1994, p. 679), using Zircaloy-4 and Zr-1%Nb samples, found about 40% tetragonal structure at the metal/oxide interface decreasing to about 15% as the distance increased. However, during investigations on Zr-2.5%Nb by Khatamian and Lalonde (1997, pp. 10-Abstract), it was determined that the oxide had a mixture of nearly-cubic tetragonal and monoclinic structures for films of 200 nm thick, or less, and a monoclinic crystal structure for the outer layers of films thicker than 800 nm. The high-stress oxide region adjacent to the base metal may be an important factor in interpreting different sets of experimental results. For example, the stresses formed in oxide films on thin strip material may relax at an early stage through strain of the base material; whereas, similar oxide stresses formed on relatively heavy wall cladding may remain and retain the tetragonal structure.

It is expected that identical zirconium or zirconium alloy samples tested under similar conditions will produce similar oxidation rates irrespective of whether the test is performed in air, water, or steam. Therefore, any corrosion rates obtained from water or steam tests can also be applied for air oxidation. This is important during the analysis of repository corrosion rates because the environment will be air or water for most of the time.

6.1.2 Temperature

Although zirconium may be considered to be a refractory metal due to its high melting point, it has the potential to react with many metallic and non-metallic elements at temperatures significantly below this value. However, at temperatures of 350°C or less, the zirconium corrosion rate does not appear to show a strong dependence on temperature when in compatible environments. As an example, the corrosion rate of zirconium changes little in nitric acid or dilute sulfuric acid as the temperature increases. With increasing temperature, the corrosion rate of zirconium may increase but so does the film formation rate. The net change in the corrosion rate remains small.

By comparison, in non-compatible media such as hydrofluoric acid and concentrated sulfuric acid, the corrosion rate of zirconium increases rapidly with increasing temperature.

6.1.3 pH

Thermodynamically, zirconium behaves like most passive metals in acidic and alkaline solutions as shown in [Figures 1a and 1b](#) (Pourbaix 1966, pp. 226 and 227). From [Figure 1a](#) and the original text, zirconium dioxide or its hydrate dissolves as ZrO^{2+} when the pH is between 3.5 and -1.03; whereas, Zr^{4+} is formed when the pH is less than or equal to -1.03. However, the dissolution rate of ZrO^{2+} is much slower than that for the Zr^{4+} ion, so zirconium dioxide films will retain most of their protective capability down to pH values of -1.03. Under alkaline conditions, the oxide protects the base metal to a pH of at least 13 as shown in [Figure 1b](#). It is, thus, concluded that the corrosion resistance of zirconium is impacted very little by change in pH over a wide range (Brown and Walton 1975, p. 324). However, pH changes may influence the composition of the local environment, for example, the presence of fluoride ions and the change from the ferrous to the ferric state as discussed below.

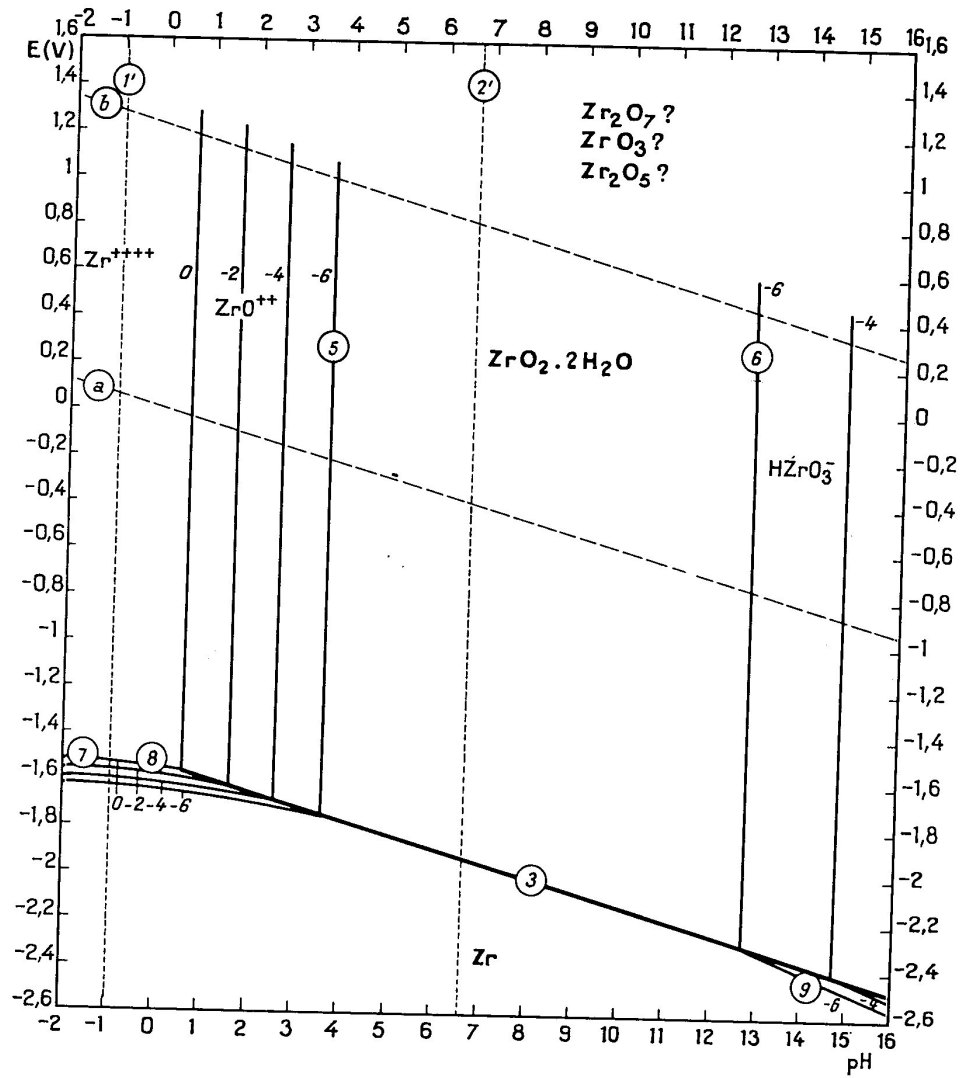
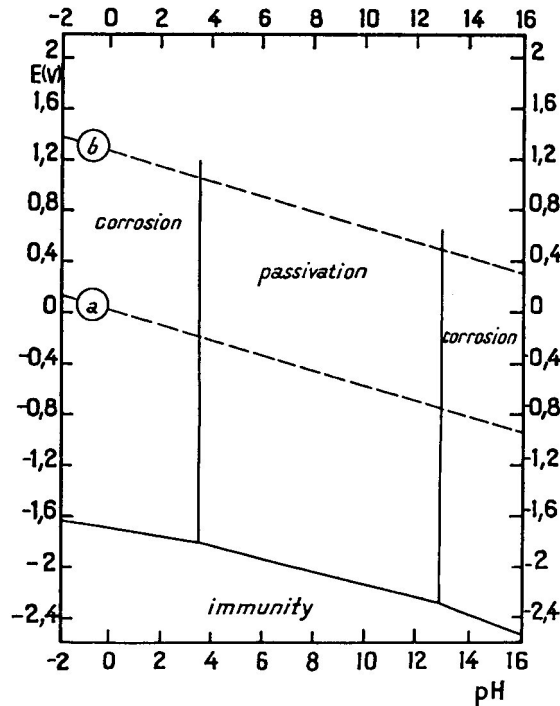


Figure 1a. The Potential-pH Diagram of Zirconium in Water at 25°C

Note: Details of the alpha-numeric symbols are from the original text of the reference (Pourbaix 1966) and are not germane to the discussion of this AMR.



NOTES: Kinetically, passivation may be extended to $\text{pH} = -1.03$. Details of the alpha-numeric symbols are from the original text of the reference (Pourbaix 1966) and are not germane to the discussion of this AMR.

Figure 1b. Theoretical Conditions of Corrosion, Immunity, and Passivation of Zirconium at 25°C

The ferric ion is a well-known oxidizing ion that can induce pitting in zirconium and its alloys when in halide solutions. Figure 2 (Pourbaix 1966, p. 313) shows that the ferric ion can exist in solution when the pH is less than or equal to 2.5 and when the potential exceeds 0.771 volts versus NHE. This condition does not normally exist since iron produces ferrous ions in acid solution, and these are too reducing to induce pitting. However, ferric ions can be produced from ferrous ions in the presence of oxygen. Under these conditions pitting can be controlled by the presence of inhibitors such as reducing agents or oxygen scavengers that prevent the formation of the ferric state (Yau and Maguire 1990, pp. 313-317). As an example, zirconium corrodes in boiling 18% HCl + 1% FeCl₂ because the ferrous ions are oxidized to ferric ions. This is visible as the solution color changes from green to brown. However, the corrosion stops when the solution is purged with hydrogen plus the addition of 1 g/l SnCl₂.

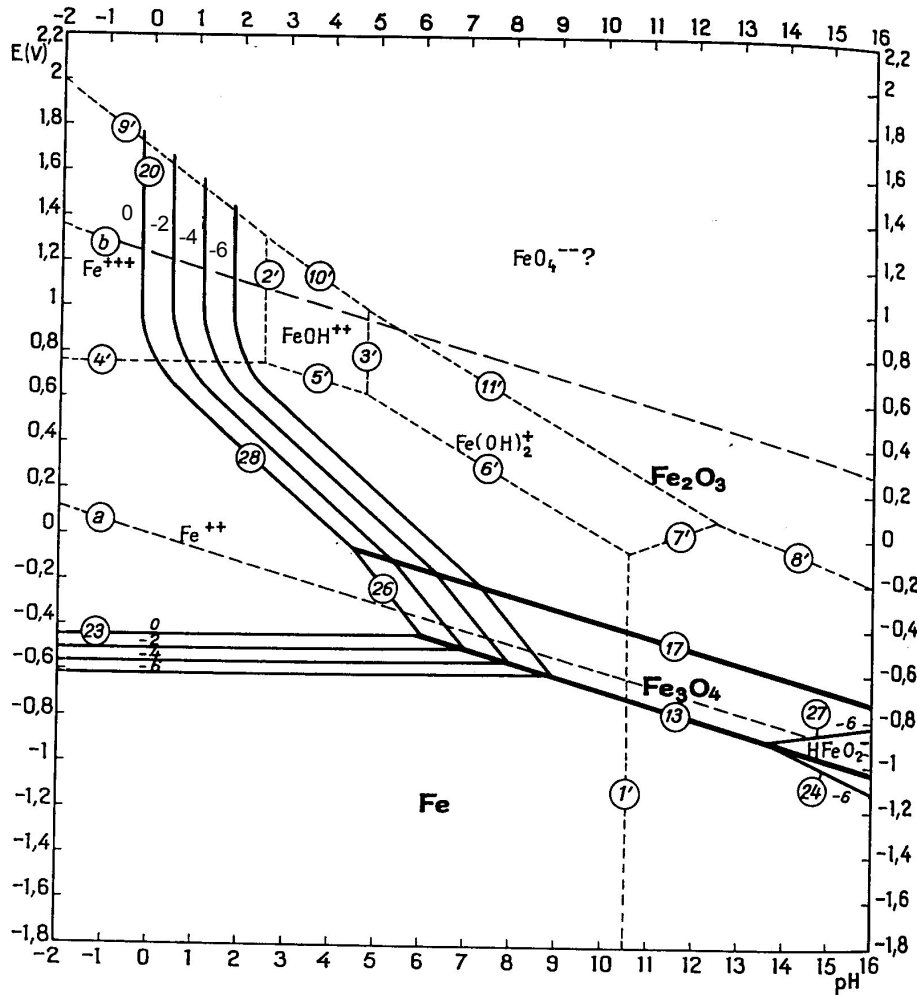


Figure 2. The Potential-pH Diagram of Iron in Water at 25°C

NOTE: Details of the alpha-numeric symbols are from the original text of the reference (Pourbaix 1966) and are not germane to the discussion of this AMR.

The fluoride ion has the capacity to interfere with zirconium oxide formation at low temperatures. The conditions under which the fluoride ion causes accelerated corrosion are complicated and depend on a number of parameters. The corrosion rate is dramatically affected by pH although hydrofluoric acid will readily dissolve zirconium metal at all concentrations and temperatures. HNO₃/HF solutions are typically used to pickle zirconium at room temperature although the dissolution rate decreases significantly as the HF concentration decreases.

Although zirconium is not resistant to HF, it has some resistance to other fluoride solutions such as calcium and sodium fluorides, provided the pH is sufficiently high and the

temperature sufficiently low. As an example, zirconium does not corrode in saturated calcium fluoride at pH 5 and 90°C. The same is true when zirconium is immersed in saturated sodium fluoride at pH 7.4 and 28°C, but the corrosion rate increases rapidly to more than 1,270 µm/yr at 90°C in the same solution. A major difference between calcium and sodium fluorides is their solubility in water. The room temperature values are 2 ppm and 4,300 ppm, respectively. These results suggest that hot solutions with a high concentration of dissolved fluoride ions can be corrosive to zirconium. It should be noted that the concentration of dissolved fluoride ions is not always proportional to the concentration of the added fluoride salt. In a mixed solution of chlorides and fluorides sharing a common cation, the solubility product, K_{sp} , of the less soluble salt cannot exceed a constant value. For example, the K_{sp} of CaF_2 , i.e., $[\text{Ca}^{+2}] \times [\text{F}^-]^2$, in water at 26°C is 3.95×10^{-11} . To maintain this value, the F^- ion concentration must decrease if the Ca^{+2} ion concentration increases. Thus, the addition of CaCl_2 will result in the precipitation of CaF_2 and a reduction in the fluoride ion concentration and, hence, in the corrosion rate as indicated in Table 6.

Table 6. Dissolved Fluoride Ions in Mixed Solutions

Solution				pH	F ⁻ in Water, ppm
CaCl ₂ , %	MgCl ₂ , %	F ⁻ (NaF), ppm	F ⁻ (CaF ₂), ppm		
0.2	0.1	200	100	1	198
0.2	0.1	200	100	3	19
2.0	1.0	200	2800	1	91
2.0	1.0	200	2800	3	18
6.6	3.3	200	9800	1	68
6.6	3.3	200	9800	3	9

Regarding the necessary conditions required for the presence of HF, Figure 3 (Pourbaix 1966, p. 583) shows that hydrofluoric acid exists when the pH is less than or equal to 3.18. Any dissolved fluoride ions will be converted to hydrofluoric acid when the pH is below this value. Under these conditions, fluoride-containing solutions can become vigorously corrosive to zirconium regardless of temperature.

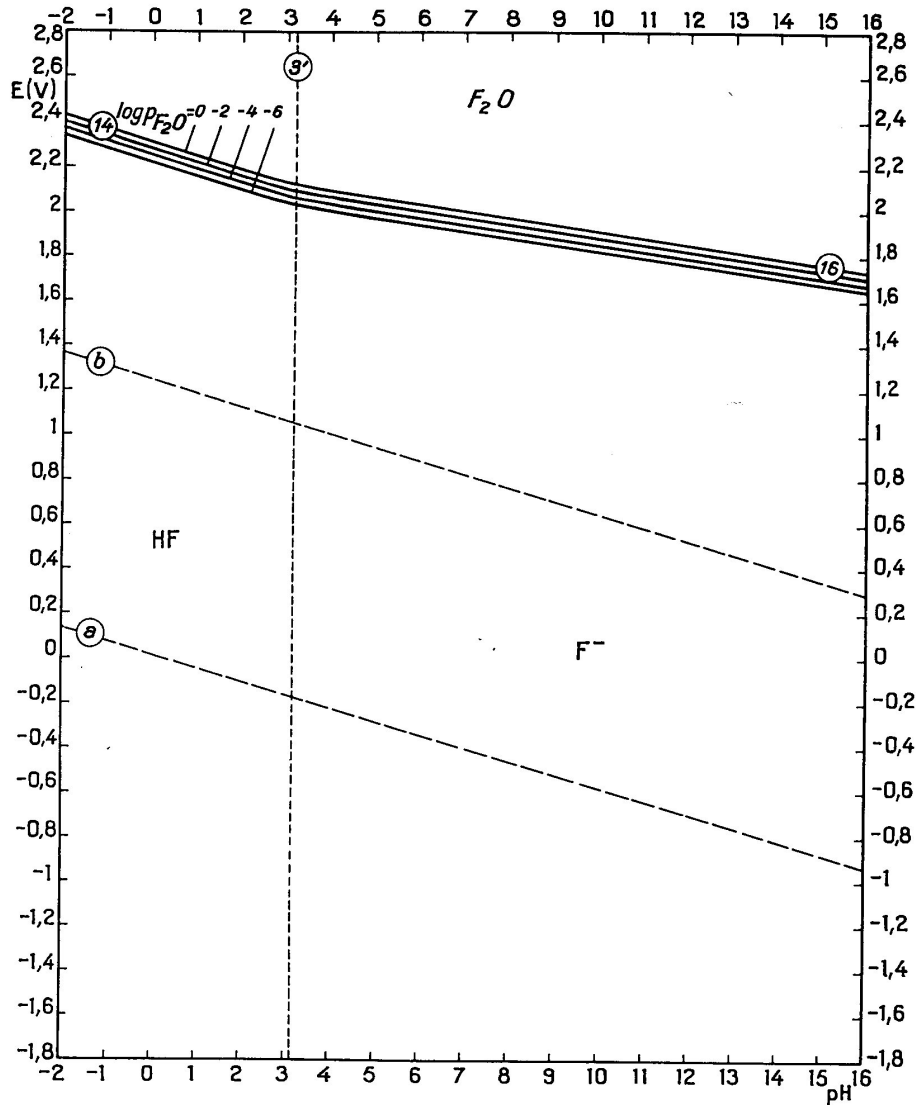


Figure 3. The Potential-pH Diagram of Fluorine in Water at 25°C

NOTE: Details of the alpha-numeric symbols are from the original text of the reference (Pourbaix 1966) and are not germane to the discussion of this AMR.

6.1.4 Water and Steam

Zirconium metal exhibits excellent corrosion resistance in steam and water at temperatures up to 350°C. It forms a protective oxide film by reaction with the water and also retains this corrosion resistance in oxidizing media such as nitric acid, and highly reducing media such as hydrochloric acid and dilute sulfuric acid. The Zr-Sn alloys, Zircaloy-2 and Zircaloy-4, also have excellent corrosion resistance, but the oxidation mechanism between the metal and alloys may be somewhat different. The metal produces a white, porous oxide film on initial oxidation; whereas, the alloys initially produce a tightly adherent black/gray oxide film at a

quasi-cubic rate. At a transition point, of the order of 2-4 micron thickness, the oxidation rate changes to linear behavior. The oxide color also changes from the black/gray to buff or white as the oxide thickness increases. With the possible exception of the bottom of fuel rods, one or more cycles of irradiation covers the length of the cladding with oxide having a thickness beyond the transition point.

There have been a number of studies of the uniform corrosion rates of Zircaloy-2 and Zircaloy-4. The longest known corrosion study was for 10,507 days (about 29 years) (Hillner et al. 1998, p. 1). Twenty-two different autoclave tests were performed with coupon specimens from 46 different Zircaloy-2 and Zircaloy-4 heats. The results of the study, which were probably on some early generation material, gave slightly higher rates than those obtained in subsequent studies by other investigators. Thus, it can be considered that the rates are bounding for uniform corrosion. Hillner's recommended equation for uniform corrosion follows:

$$\Delta\Delta W = 3.47 \times 10^7 \exp\{-11452/T\} \times \Delta t \quad (\text{Eq. 1})$$

where

$\Delta\Delta W$ = specimen weight gain in units of mg/dm^2

T = absolute temperature in units of K

Δt = exposure time, in units of days

Note that one micron of oxide thickness is approximately $15 \text{ mg}/\text{dm}^2$ weight gain.

Regarding the corrosion performance of other nuclear grade zirconium alloy compositions, Zr-2.5Nb generally has a higher corrosion rate than the Zircaloys but appears to be superior to Zircaloy-2 at high temperatures, 500°C (Dalgaard 1962, p. 176).

As noted in Attachment III.1, unalloyed zirconium appears to show variable corrosion performance in pure water. This variability is not observed in less pure water. This is a benefit since city water, river water, and seawater are frequently used as the cooling medium in the CPI. Although these sources have much higher impurity levels than "nuclear grade" water, zirconium has still provided excellent corrosion performance for periods in excess of 20 years and at temperatures around 300°C .

6.1.5 Halides

Zirconium resists attack by most halides, including halogen acids. The major exceptions are hydrofluoric acid, ferric chloride, and cupric chloride. As shown in Section 6.1.3, zirconium is corrosion resistant to certain fluorides when the pH is sufficiently high. Low fluoride ion concentrations, on the order of a few ppm, in city or ground water have little effect on zirconium's excellent corrosion resistance. However, a few ppm of hydrofluoric acid will noticeably increase zirconium's corrosion rate.

The presence of acidic fluoride solution is not always bad for zirconium since fluoride can counteract the effect of oxidizing agents. Chemically, it can make an oxidizing solution less oxidizing or even reducing. Consequently, the presence of fluorides in an acidic chloride

solution makes zirconium less vulnerable to pitting and SCC (Yau and Macguire 1990, p. 317).

The corrosion resistance of zirconium in halides increases in the order chloride, bromide, and iodide. Unless the environment is oxidizing, zirconium is very corrosion resistant in chloride solutions, including strong hydrochloric acid. Oxidizing conditions include the presence of oxidizing agents, coupling with a noble material and applied anodic potential.

Zirconium corrosion in chloride solutions is also discussed in Sections 6.1.9 and 6.1.11. Zirconium corrosion in bromide or iodide solutions is minimal, and neither is addressed in this report due to the absence of these elements in the repository.

6.1.6 Nitrates

Although zirconium is normally susceptible to pitting in acidic oxidizing chloride solutions, the nitrate ion, NO_3^- , is an effective inhibitor against zirconium pitting (Andreeva & Glukhova 1961, p. 395; Andreeva and Glukhova 1962, p. 468; Jangg et al. 1978, p. 16; Maraghini et al. 1954, p. 407) because of its passivating power. The minimum $[\text{NO}_3^-]/[\text{Cl}^-]$ molar ratio required to inhibit pitting of zirconium was determined to be one (Andreeva and Glukhova 1961, p. 395; Jangg et al. 1978, p. 19) or five (Maraghini et al. 1954, p. 406). However, it is recommended that high concentrations of HCl be avoided since zirconium is not inert to aqua regia.

6.1.7 Silicon Dioxide

The major source of zirconium is Zircon. This is a combination of zirconium dioxide and silicon dioxide and is extremely inert. Ideally, it would be beneficial if the silicon dioxide present in most natural waters reacted with the zirconium oxide to form a zirconium silicon-oxide film. Theoretically, this composition would be even more corrosion resistant than the zirconium oxide film.

Although frequently used as a corrosion-resistant coating on materials, silicon dioxide reacts with hydrofluoric acid to form fluosilicic acid. Since fluosilicic acid is highly corrosive to zirconium even at room temperature, silicon dioxide cannot be used as a technique to prevent attack of zirconium by acidic fluorides. One technique to protect zirconium products is the use of more reactive forms of zirconium such as sponge or zirconium chemicals, to complex fluoride ions more quickly (Yau and Maguire 1990, p. 317). For example, the corrosion rate of zirconium in 90% HNO_3 + 200 ppm HF at 25°C is greater than 25,400 $\mu\text{m}/\text{yr}$. By adding 800-ppm zirconium sponge into the same solution, the corrosion rate is lowered to 25.4 $\mu\text{m}/\text{yr}$. Also, the susceptibility of zirconium to SCC in 90% HNO_3 is eliminated. Results of short-term tests show that Zircaloy shavings corrode at rates approaching 3,000 $\mu\text{m}/\text{yr}$ in 1,000-ppm fluoride-containing solutions over a temperature range of 21.5°C to 56.5°C when the pH is between 5 and 6. The rates become much lower (0.03 to 0.3 $\mu\text{m}/\text{yr}$) when the pH is around 8 (Uziemblo and Smith 1989, pp. 12, 18).

6.1.8 Sulfur and its Compounds

Sulfur and its compounds are highly corrosive to common metals. They are often present in underground fluids such as oil, natural gas, and geothermal fluids. Though zirconium is a reactive metal, it has very little affinity for sulfur (Blumenthal 1969, p. 65). Consequently, zirconium has excellent corrosion resistance to sulfur and its compounds. It is not expected that zirconium will react with sulfur vapor or hydrogen sulfide below 500°C (Yau 1983, pp. 191-2). In addition, there is no instance of zirconium-sulfur bonds forming in aqueous systems (Blumenthal 1969, p. 65; Latimer 1952, p. 272).

Many metals and alloys produce complicated reactions with sulfuric acid. This is due to the reducing nature of the acid in dilute solution and its oxidizing nature when concentrated. By contrast zirconium is very resistant to corrosion at all concentrations up to 70% and at temperatures above boiling. In 70 to 80% concentrated sulfuric acid, the corrosion resistance of zirconium depends strongly on temperature. At even higher concentrations, the corrosion rate of zirconium increases rapidly due to the formation of non-protective zirconium sulfate film. These affects are shown in Figures 4 to 6.

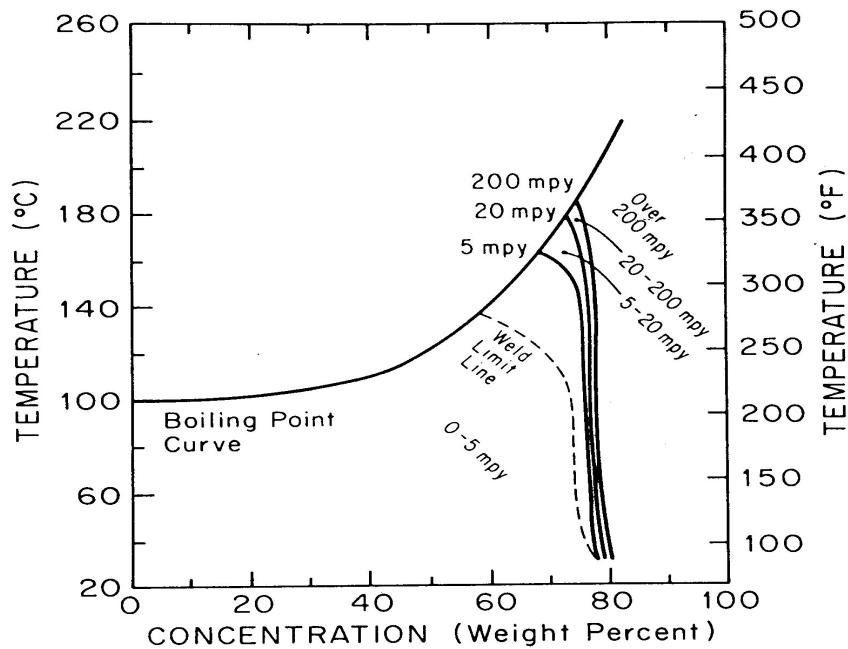


Figure 4. The Iso-Corrosion Diagram of Zr 702 in Sulfuric Acid

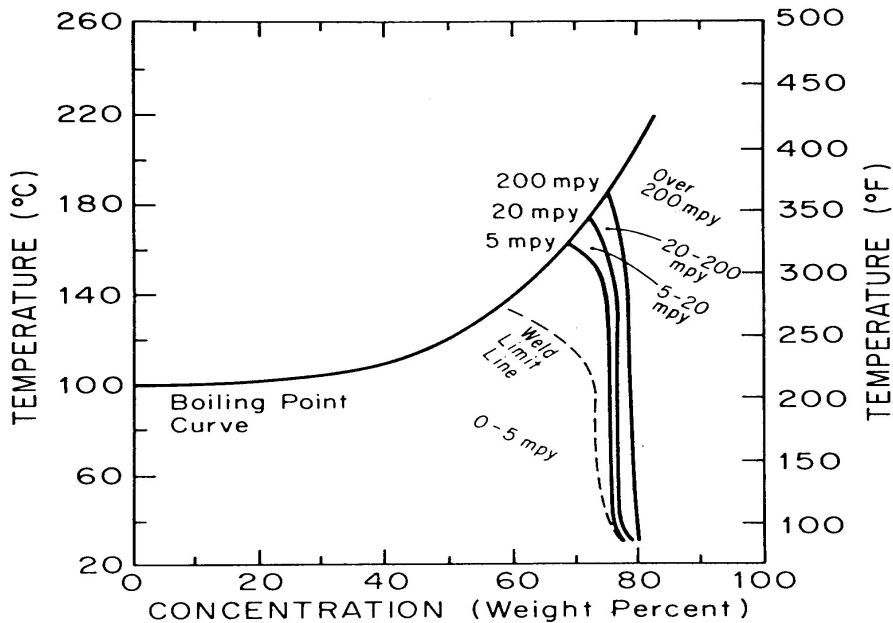


Figure 5. The Iso-Corrosion Diagram of Zr 704 in Sulfuric Acid

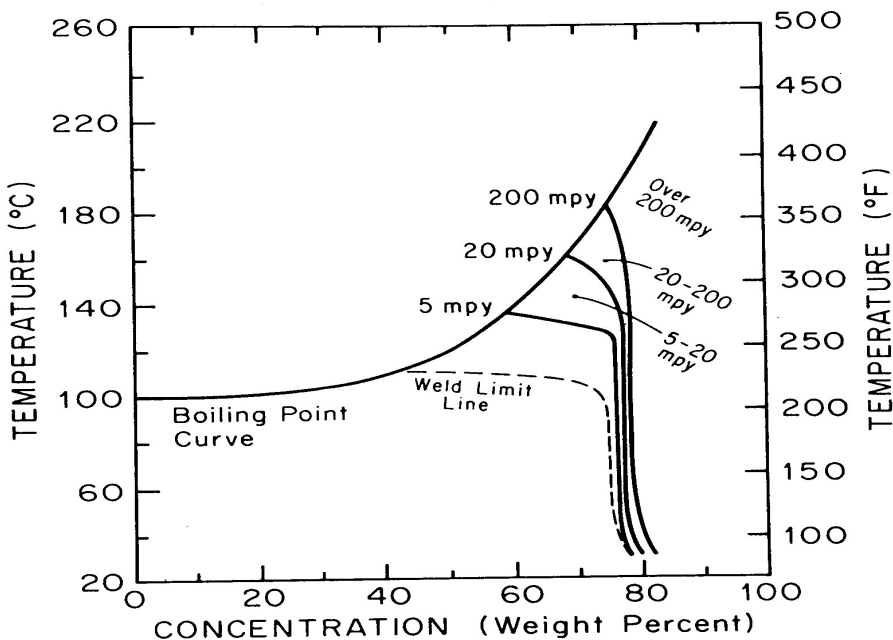


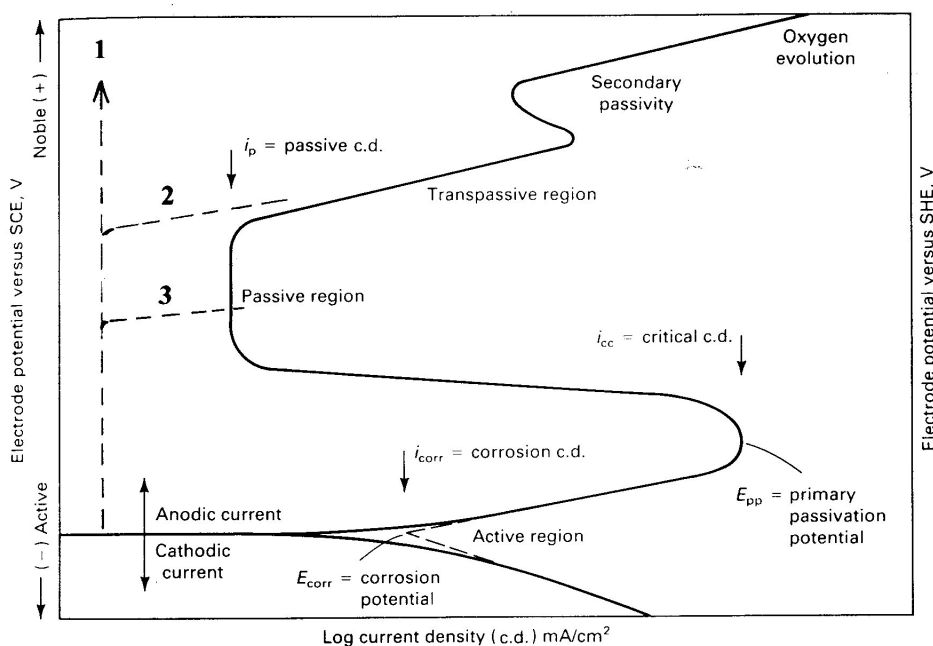
Figure 6. The Iso-Corrosion Diagram of Zr 705 in Sulfuric Acid

The sulfate ion has a mild inhibitive effect on the pitting of zirconium in chloride solutions. In a 0.01 M chloride solution, a minimum $[\text{SO}_4^{2-}]/[\text{Cl}^-]$ ratio of 54 is reported for inhibition, but this ratio decreases to 42 in a 1% chloride solution (Yau and McGuire 1990, pp. 314-316).

This means that the higher the sulfate ion concentration, the greater the ferric ion concentration that can be tolerated before zirconium pitting occurs.

6.1.9 Pitting

Zirconium is susceptible to pitting in all halide solutions except fluoride. In fluoride solutions zirconium is vulnerable to general corrosion. Figure 7 illustrates the electrochemical behaviors of zirconium and stainless steel. In halide-free solutions, zirconium has greater corrosion resistance than stainless steel and most other passive alloys. In halide-containing solutions, zirconium's advantage disappears under oxidizing conditions. It may have a slightly higher pitting potential than stainless steel, but zirconium pits at a much higher rate under a constant potential condition.



NOTE: Solid line: Common Features Found in Stainless Steel
 Dashed Line: Common Features Found in Zirconium
 1: In Halide-free Dilute Solutions
 2: In Halide-free Concentrated Solutions
 3: In Halide-containing Solutions

Figure 7. The Electrochemical Behaviors of Stainless Steel and Zirconium

Zirconium's pitting susceptibility is greatest in chloride solutions and decreases as the halide ion becomes heavier. The reverse is true for titanium and tantalum. The pitting potentials of zirconium in 1N solutions of Cl^- , Br^- , and I^- are 380, 660, and 910 mV_{NHE} , respectively. These potentials decrease gradually with increasing concentration and rapidly in concentrated halide solutions (Macguire 1984, pp. 181). Other factors such as pH (Macguire, pp. 184), temperature (Macguire 1984, p. 184), alloying element (Cragolino and Galvele 1978, p. 1056), and film quality (Shibata and Ameer 1992, p. 1637) also affect pitting potential.

With the exception of acidic chloride solutions, zirconium does not pit in halide solutions because its corrosion potential is often lower than the pitting potential. The presence of oxidizing ions such as ferric and cupric ions, in acidic chloride solutions may increase the corrosion potential to exceed the pitting potential in which case pitting may occur. The standard potentials of several reduction/oxidation pairs are given in Table 7.

Table 7. Reduction/Oxidation Pairs

Reduction/Oxidation Pair	Mv, NHE
$\text{Am}^{4+} / \text{Am}^{3+}$	2,180
$\text{H}_2 \text{O}_2 + \text{H}^+ / \text{H}_2\text{O}$	1,770
$\text{Cl}_2 / \text{Cl}^-$	1,360
$\text{Pd}^{2+} / \text{Pd}$	987
$\text{Pu}^{4+} / \text{Pu}^{3+}$	970
$\text{Fe}^{3+} / \text{Fe}^{2+}$	771
Cu^+ / Cu	521
$\text{Cu}^{+2} / \text{Cu}$	337
$\text{Cu}^{+2} / \text{Cu}^+$	153
$\text{Sn}^{4+} / \text{Sn}^{2+}$	150
H^+ / H_2	0.0
$\text{Sn}^{2+} / \text{Sn}$	- 136
$\text{Fe}^{2+} / \text{Fe}$	- 440

Pitting may also occur when there is an applied anodic potential or when zirconium is coupled with a noble material such as graphite or platinum. Pitting caused by these conditions is not considered in this report because the potential for this scenario is considered very low.

To cause pitting in zirconium, the oxidizing power needs to be stronger than that of the cupric ion. There must also be sufficient oxidizing ions in the chloride solution for pitting to occur. According to the mixing potential theory, the solution potential does not reach or exceed the pitting potential when there are insufficient oxidizing ions. Below the minimum, the presence of oxidizing ions may actually enhance the protective oxide formation process. The minimum amount of oxidizing ions required to induce pitting appears to depend on the chloride concentration, pH, temperature, and other factors. The values are not firmly established but appear to be ranging from a few ppm in concentrated hydrochloric acid to 1,000's ppm or more in dilute chloride solutions.

Pit initiation is complicated and not well understood. It appears to be the result of a unique type of anodic reaction. After the initiation stage, a model for the corrosion process within a pit is shown in Figure 8 (Fontana 1986, p. 52). A metal M pits in an aerated sodium chloride solution. Rapid dissolution occurs within the pit, while oxygen reduction takes place on adjacent surfaces. In the presence of ferric ions, the reduction of ferric ion to ferrous ion is an "addition reduction reaction". The rapid dissolution of metal within the pit tends to produce an excess of positive charge in this area, resulting in the migration of chloride ions to maintain electroneutrality. Thus, in the pit there is a high concentration of metal chloride. As the result of the hydrolysis of metal chloride, a high concentration of hydrogen ions is created. Both hydrogen and chloride ions stimulate the dissolution of most metals and alloys, and the pitting growth rate increases with time. However, as discussed in Sections 6.1.3 and 6.1.5, these conditions are not particularly harmful to zirconium. After creation of the pit, the conditions become increasingly favorable for zirconium because it has the ability to form a

protective oxide film in reducing acids. After the reduction of some oxidizing ions, the driving force for pitting decreases with time. Eventually, the pitting process stops due to the oxide formation at the pit, and zirconium is observed to have shallow pits covered with oxide films. Due to zirconium's ability to produce an oxide in low pH solutions and the ability of the oxygen to migrate, the protective oxide film is formed where needed. Pitting stops when the driving force weakens. As was shown while monitoring pitting by electrochemical noise technique, the pitting process slows down and then stops as the ferric chloride solution is diluted (Fahey et al. 1997, p. 55).

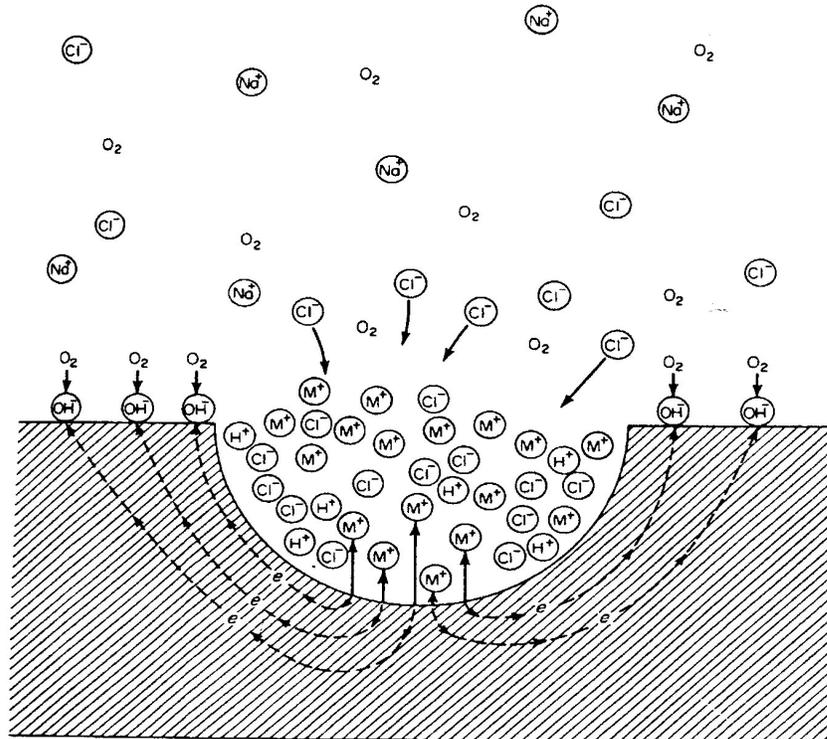
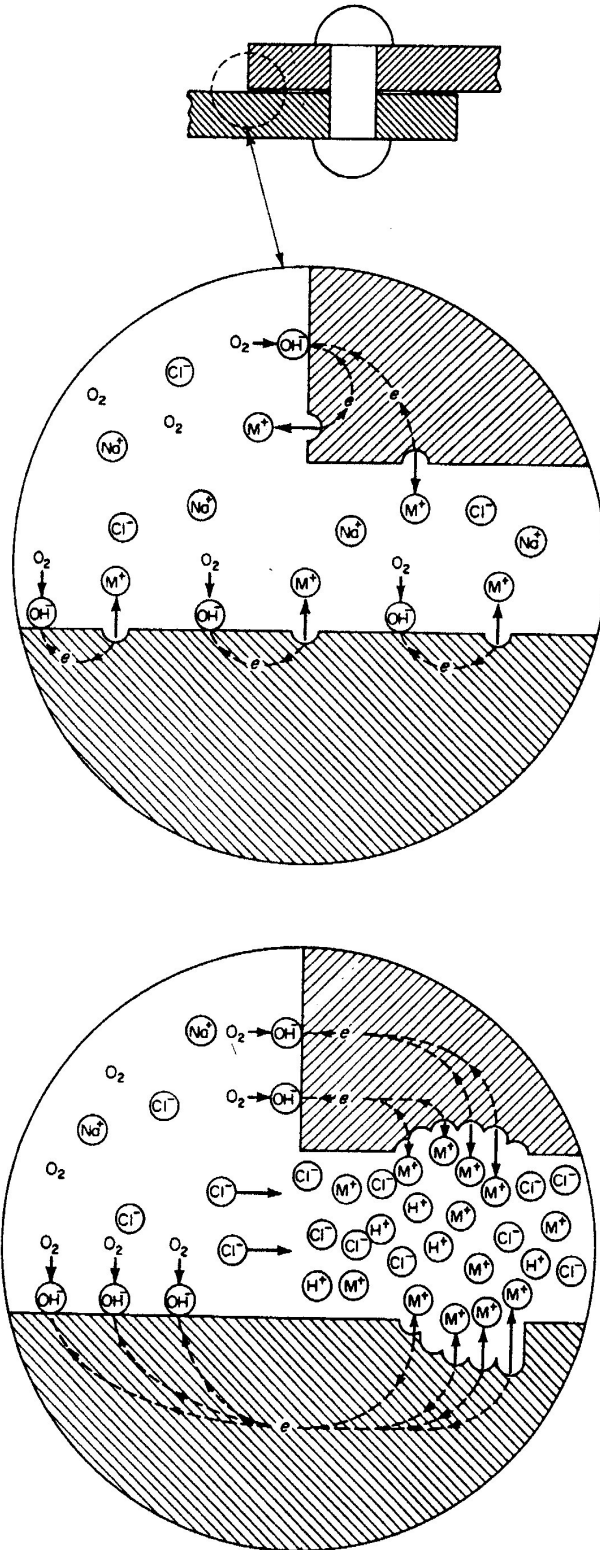


Figure 8. The Corrosion Process within a Pit

If zirconium pitting is caused by an applied potential or by galvanic coupling, the pit will continue to grow. At a constant potential above the pitting potential, the pit generation rate is always higher than the pit repassivation rate (Shibata and Ameer 1992, p. 1642).

6.1.10 Crevice Corrosion

Zirconium is one of the most crevice corrosion resistant materials. For example, it is not subject to crevice corrosion even under such adverse conditions as low-pH chloride solutions or wet chlorine gas. This can be rationalized by the model for crevice corrosion as shown in Figure 9 (Fontana 1986, pp. 42-43).



NOTE: Top: Initial Stage—Bottom: Later Stage

Figure 9. Crevice Corrosion

Initially, metal dissolution and oxygen reduction occurs uniformly over the entire surface, including the interior of the crevice. After a short interval, the oxygen within the crevice is depleted because of the restricted convection, so oxygen reduction ceases within the crevice; however, metal dissolution continues. This tends to produce an excess of positive charge in the solution that is necessarily balanced by the migration of negative chloride ions into the crevice. At the same time, positively charged ions such as the ferric ion, Fe^{3+} , tend to stay outside the crevice. In addition, the condition within crevices is too reducing to have ferric ions. Similar to the pitting process, metal chloride dissociates into an insoluble hydroxide and a free acid ($\text{H}^+ + \text{Cl}^-$). Again, these changes do not affect the zirconium corrosion. Consequently, zirconium is not susceptible to crevice corrosion in chloride solutions. As detailed in Section 4.1, crevice corrosion and SCC tests have been performed to determine whether crevice corrosion does occur in low pH-chloride solutions with ferric ions. No crevice corrosion has been observed in these or other tests.

If the same model were used for the fluoride situation, then zirconium would be considered susceptible to crevice corrosion in fluoride solutions. Crevice corrosion at the contact between zirconium and PTFE would be a special case. PTFE is an inert material and releases few fluoride ions when manufactured by the pressurized process. However, it can also be produced from recycled materials by remelting. Recycled PTFE is not as stable as virgin PTFE and can release large amounts of fluorides. Crevice corrosion of zirconium under PTFE gaskets has occurred several times in acids when recycled PTFE or a less stable type of fluoropolymer has been used. These observations support the model.

6.1.11 Stress Corrosion Cracking

Yau (1992, pp. 299-311) provides significant details on the conditions required to produce SCC in zirconium alloys. The metal and alloys resist SCC in many aggressive environments, including NaCl, MgCl_2 , NaOH, and H_2S , which are considered strong SCC-inducing agents for a number of metals and alloys. The high SCC resistance of zirconium is attributed to its high repassivation rate. Any breakdown in the surface oxide film is quickly healed in an oxidizing environment.

The environments known to cause SCC in zirconium include FeCl_3 , CuCl_2 , halogen or halide-containing methanol, concentrated HNO_3 , liquid mercury or cesium (Yau 1992, p. 303), and 64 to 69% H_2SO_4 (Fitzgerald and Yau 1993, p. 1).

Measures utilized to prevent SCC in zirconium include the following:

- Avoiding high sustained tensile stresses
- Modifying the environment, e.g., changing pH, concentration, or adding an inhibitor
- Maintaining a high-quality surface film, i.e., one low in impurities, defects, and mechanical damages
- Applying a small cathodic potential

- Insulating the contact between zirconium and a noble material such as graphite and platinum
- Shot peening.

6.1.12 Surface Condition

Corrosion is a surface phenomenon, and the zirconium corrosion rate is affected by the surface condition (Thomas 1955, p. 619; Kass 1964, p. 5). Layers of disturbed metal from mechanical operations tend to produce higher oxidation rates and significant benefits can be achieved from chemically pickling the surface. The corrosion resistance of zirconium does not appear to be affected by common surface features such as scratches or heat tint but may be degraded by embedded particles such as silicon carbide when in oxidizing chloride solutions.

Figure 10 (Yau and Macguire 1990, p. 312) shows the effect of surface condition on the rest potential of zirconium (Zr702) in 10% HCl + 500 ppm Fe^{3+} at 30°C. Air annealing yields rest potentials nobler than the pitting potential, E_{crit} , due to the thick oxide formed during annealing. This does not mean that pitting will occur if the film quality is good, but it does put thick oxide-coated materials in a position vulnerable to pitting, particularly when there is an anodically applied potential. Surfaces abraded with either 600 grit SiC or Al_2O_3 cloth reach the pitting potential quickly and have short pit initiation times due to the presence of embedded particles from rough polishing. Pickled and finely polished surfaces have rest potentials below the pitting potential. They are very resistant to pitting even in oxidizing chloride solutions. This can be attributed to surface homogeneity that favors general corrosion but not localized corrosion. Results of immersion tests confirm these exceptions (Yau and Macguire 1990, p. 312; Fahey et al. 1997, p. 57). It should also be noted that cladding destined for the repository will be covered with a thick oxide, which is an inert insulator and, therefore, not a good substrate for electrochemical reactions.

Further evidence of the significant benefits of pickling on general corrosion and pitting of zirconium can be seen in Section 4.1.1. Test 3. This effect has been long recognized in the nuclear industry, and advantage is taken of the phenomenon by pickling cladding prior to use.

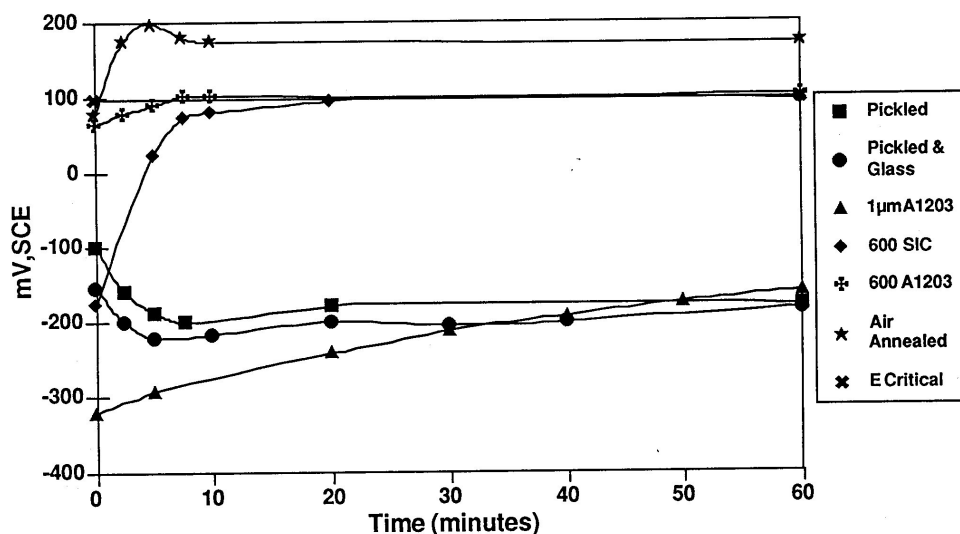


Figure 10. Surface Effect on the Rest Potential of Zr 702 in 10% HCl Plus 500 ppm Ferric Ion at 30°C

6.1.13 Alloying Elements

Zirconium is miscible only with titanium, hafnium, and scandium and does not readily form alloys with other elements. Since most elements have low solubilities in zirconium and form brittle intermetallic compounds, all commercial zirconium alloys are low in alloy content. However, all the alloys are highly corrosion resistant over a wide range of media and show relatively little variability between the alloys in their corrosion resistance. The corrosion rates of different zirconium alloys in sulfuric acid provide an example. Figures 4 to 6 show the corrosion rates for Zr 702, Zr 704, and Zr 705 in sulfuric acid. There is little to differentiate the performance of these three alloys since all show high corrosion resistance in < 70% concentration acid and poor corrosion resistant in > 70% concentration acid.

Differences between the alloys exhibit themselves in the 60 to 70% acid concentration range. Within this range, Zr 702 is the most corrosion resistant and Zr 705 is the least resistant. This order can change in other environments. For example, Zr 705 shows the best corrosion resistance in steam at temperatures above 400°C and in certain organic acids. Similarly, Zircaloy-2 and Zircaloy-4 show different corrosion characteristics at high temperatures, typically in excess of 400°C, but the behavior of the two alloys is essentially the same at lower temperatures.

Electrochemically, Zr 702 (commercial grade zirconium) and Zircaloy-4 behave similarly in NaCl solutions although the pitting potential of Zr 702 has been measured at 34 Mv higher than that for Zircaloy-4 (Cragolino and Galvele 1978, p. 1053). Zr 702 and Zircaloy-4 are close in corrosion resistance in chloride solutions.

6.1.14 Irradiation

Zirconium has greater resistance to radiation damages than most metals and alloys, possibly due to its low-thermal-neutron cross section. However, irradiation does cause some effects that are not observed under non-irradiated conditions. The most noticeable effect is

irradiation-induced growth. Cladding has shown fuel-rod length increases and diameter decreases of 1% or greater at high burnups (Holzer and Stehle 1986, p. 28).

Irradiation can also produce metallurgical changes. In Zircaloy-2, the iron in the $Zr(Cr,Fe)_2$ precipitates, and both the iron and nickel present in the $Zr_2(Ni,Fe)$ precipitates dissolve into the matrix (Etoh et al. 1991, p. 696). The overall effect is an improvement in the nodular corrosion resistance of Zircaloy-2 (Etoh et al. 1991, p. 691; Etoh et al. 1992, p. 45). The solute redistribution into the alloy matrix and subsequent control of nodular corrosion was supported in a later work by Cheng et al. (1994, p. 414) with the belief that the phenomenon occurs in both Zircaloy-2 and Zircaloy-4. It should be noted that these studies focused on the impact of microstructural changes on nodular corrosion, which is believed to only occur in Zircaloys under boiling conditions. Under repository conditions, uniform corrosion is assumed and, as quoted by Hillner et al. 1998 (p. 13), "... it was found that corrosion rates decreased with annealing and precipitation of these alloying elements, with the optimum amount depending on the in-service conditions."

Irradiation effects on the general corrosion and oxidation of Zircaloys in water have been reported by Stehle et al. (1984, p. 484). They observed that the PWR environment enhanced the corrosion rate by up to about three times that expected from ex-reactor testing. The enhancement factor varied from reactor to reactor and within a given reactor from cycle to cycle. The oxide-film thermal conductivity and coolant chemistry were identified as major factors influencing the corrosion behavior. It is generally believed that the in-core corrosion acceleration is caused by the fast neutron component of the flux and, since this is very low in the repository, no corrosion enhancement is expected under repository conditions.

No reports have been found on the effects of irradiation on the pitting of zirconium and its alloys in halide solutions. However, since irradiation tends to produce a more homogeneous microstructure, the effects of irradiation should not be deleterious.

6.2 ZIRCONIUM CORROSION—EXPERIMENTAL DATA

6.2.1 Uniform Corrosion of Zirconium and its Alloys

The corrosion resistance of the nuclear grade zirconium-tin alloys, commonly known as Zircaloys, has been determined from long-term corrosion tests in water, in steam, and from in-reactor performance. Based on data obtained over a 29-year experiment, Hillner et.al. (1998, p. 7) concluded that the cladding would still be intact from general corrosion after one million years. This assessment was based on predicted repository temperatures at Yucca Mountain and the demonstrated low uniform corrosion rate predicted under wet or dry conditions that might be generally expected in the repository.

The equation recommended for the uniform corrosion of cladding follows:

$$\Delta\Delta W = 3.47 \times 10^7 \exp[-11452/T] \times \Delta t \quad (\text{Eq. 2})$$

where

$\Delta\Delta W$ is the weight gain in mg/dm^2

Δt is the exposure time for corrosion in days

T is the absolute temperature of the metal/oxide interfacial in Kelvin.

6.2.2 Accelerated Corrosion of Zirconium and its Alloys

There are certain chemical forms that can rapidly degrade zirconium and its alloys through localized corrosion. The following sections discuss these conditions, but they do not assess the probabilities that such adverse conditions will exist in the repository. The approach taken has been to define the environmental conditions under which these chemical forms can exist and to note these forms as potential failure modes.

In the case of the ferric ion, the above approach alone was taken. The corrosion rates in the presence of ferric ions were so high and variable that failures could, in some cases, be predicted in less than a year.

In the case of halide contamination, the same approach was initially taken, i.e., that of defining the conditions under which fluoride ions can exist, but an effort was also made to empirically correlate the observed corrosion rates with the experimental fluoride and chloride concentrations. This latter effort was partially successful, but there appears to be a number of scenarios where the predictions are inconsistent with theory possibly due to one or more of the following:

1. Most corrosion rates are represented by a single experimental result for each test condition. No experimental conditions were represented by more than two results. The uncertainty in each value is not known but is generally estimated at 10 to 20% based on a comparison between standard deviations and experimental results. This casts some doubt on the reliability of any correlations. Further, the fact that the experimental test periods were of short duration, 64 days maximum except for the 275-day seawater test, makes the derivation of annual (or longer) corrosion rates questionable.
2. The composition of the zirconium alloy may influence the results. For example, Section 4.1.3, Tests 1 through 5 show weight gains for Zr 702 and weight losses for Zr 705. Section 4.1.3 Test 7 also shows a weight gain for Zr 702 but a weight loss for Zircaloy-2. This suggests that Zr 702 and Zr 705 data should not be combined.
3. The surface treatment (finish) of the sample can have a significant impact on the corrosion results as shown by the pickling test data in Section 4.1.1 Test 3. A similar correlation was also noted by Kass (1964, pp. 5, 6) and by Thomas (1955, p. 612). Since there are no assurances that the surface treatments or finishes were the same for all samples in these tests, a direct comparison of the results is questionable.
4. In many cases the effects of small changes in the corrosion environment can cause big, inconsistent changes in the corrosion rates. The simplest example is the accelerated

corrosion due to ferric chloride. The rate can be very high when the pH is below 2.5, but above this value, the rate approaches zero very rapidly because the ferric ion reverts to the ferrous state. It is unlikely that an empirical correlation would detect such an abrupt change without a vast database. Similarly, the corrosion rates associated with fluoride ions may well be determined by the degree of ion dissociation. Thus, a sodium fluoride solution might be expected to cause greater corrosion than calcium fluoride for the same fluoride concentration.

In summary, there are many variables and uncertainties that can affect an empirical correlation. These are discussed in the following sections.

6.2.2.1 Ferric Chloride

Contact with ferric chloride can produce pitting in zirconium and its alloys. As seen in [Figure 2](#), the ferric ion is the stable form of iron at pH values below 2.5 (25°C). Above this value the ferrous ion is the stable form and ferrous iron causes no enhancement in zirconium corrosion rates. As a first approximation, it can be stated that accelerated corrosion or pitting from ferric chloride will not occur if the pH is maintained above 2.5. In the event that the pH decreases to a value below 2.5, it is also necessary to assess whether the local potential exceeds 0.771 volts versus the NHE as discussed in Section 6.1.3.

It is noted that the highly concentrated J-13 well water has, in addition to the high pH values, sufficient sulfate and nitrate ion concentrations to suppress the pitting of zirconium. Pitting and crevice corrosion would not be a concern for zirconium and its alloys under conditions defined in Attachment III.4.

Examination of Section 4.1.1 Tests 2, 3, 9, and Section 4.1.2 suggests that ferric chloride can produce very high corrosion or pitting rates, certainly in excess of the 5-6 micron per year, which would result in through-wall failure in less than 100 years. There are two notable exceptions:

1. Section 4.1.1 Test 3 indicates that the surface finish has a significant impact on the corrosion rate decreasing from 533 micron per year for the as-received condition to 0.0 micron per year for surfaces that have been pickled for 3 or 4 minutes. Since SNF cladding is invariably pickled, it might be concluded that ferric chloride would have minimal impact on the Zircaloy corrosion. However, the duration of these tests was only 4 days, and longer test periods may have resulted in a weight loss even for the pickled surfaces.
2. Section 4.1.2 provides general corrosion and pitting rates under various HCl strengths, ferric ion concentrations, and temperatures. The test durations were longer than for most of the other tests, and the data might, therefore, be considered more reliable. The results indicate that the corrosion and pitting rates may be in the acceptable range provided the HCl concentration is 20% or less, the ferric ion concentration is 50 ppm or less, and the temperature is less than 60°C. Of the thirty-six values quoted for general corrosion, parent metal pitting and weld metal pitting, thirty-three results are 0.0 micron per year. The three remaining values are 0.1, 0.3, and 0.5 micron per year.

This data demonstrates that low ferric ion concentrations (50 ppm) can be present and not cause rapid corrosion although the rate may be temperature dependent, and the test value of 60°C may be too low for application to the repository conditions.

In summary, the following criteria are recommended for assessing the potential for accelerated corrosion from ferric ions:

- Accelerated corrosion will not occur if the pH is above 2.5. Under these conditions the ferric ion is unstable. Additional data can be obtained by reference to Pourbaix's (1966) criteria.
- If the pH value is below 2.5, the local potential must exceed 0.771 volts versus the NHE for ferric ions to be present; otherwise, the corrosion rate is not impacted.
- If ferric ions are present but the concentration is low (50 ppm or less), the HCl concentration is 20% or less and the temperature is 60°C or less, there is no apparent acceleration of the corrosion rate.
- If ferric ions are present due to a combination of low pH, high local potential, high HCl concentration, and elevated temperature, the corrosion rate is predicted to be in excess of 5 micron per year. This implies failure in less than 100 years, provided the environmental conditions remained static or deteriorated over the entire period.

6.2.2.2 Halide Reactions—Fluoride-Free Solutions

Since the minimum PWR clad wall thickness is greater than 500 micron, a corrosion rate greater than five micron per year (0.005 mm/year) may be considered as unacceptable from an integrity aspect since failure would occur in less than 100 years. Corrosion rates will initially be compared against this criterion.

Zirconium and its alloys are extremely corrosion resistant to saturated chloride solutions at temperatures up to at least 250°C. This is demonstrated by the results in Section 4.1.1, Tests 4 through 8, which all show zero or positive weight gains for Zr 702, Zr 705, Zircaloy-2, and Zircaloy-4. Changes in temperature or pH have little impact on this excellent corrosion resistance, provided the pH is at least one. Under these conditions, the passive film existing on the zirconium alloys has very low solubility, and the corrosion rate may be considered to be that of Zircaloy in water or steam. This scenario was examined by comparing the chloride corrosion rates with those reported by Hillner et al. (1998, p. 6). Hillner provides a corrosion rate for the early stages of the post-transition corrosion of:

$$\Delta\Delta W = 2.46 \times 10^8 \exp[-12877/T] \times \Delta t \quad (\text{Eq. 3})$$

Taking the conditions of Section 4.1.1 Test 5 as representing the highest test temperature and substituting this temperature, 250°C, and time, 1,824 hours, the predicted weight gain is 0.12 micron per year. This value is of the same order of magnitude as the results obtained in Section 4.1.1 Test 5, specifically 0.15, 0.48, and 0.18 micron per year weight gain for the

three non-welded conditions. It is concluded that the chloride conditions do not affect the predicted corrosion rates, and the proposed uniform oxidation model is applicable.

6.2.2.3 Halide Reactions–Fluoride-Containing Solutions

6.2.2.3.1 Data Analysis

Zirconium and its alloys have poor resistance to general corrosion in fluoride-containing solutions. However, as detailed in Section 4.1.2, pitting is not a problem being generally restricted to ferric chloride solutions.

The corrosion results presented in Section 4.1.1 were examined, and those with exposure to measured amounts of fluoride were considered for use in a correlation. These results are those from Tests 10 through 13. The results from Tests 10 and 11 were excluded because the pH was not known. The first, fifth, and ninth rows of Table 2 were also excluded because the fluoride concentration was zero, and the intention was to fit to the logarithm of the fluoride concentration. The remaining 21 observations from Tests 12 and 13 (Tables 1 through 3) were used. A linear least squares fit to these observations produced the following correlation:

$$\log_{10}(\text{corrosion rate}) = -10.40 + 4430 / T - 0.758 \cdot \text{pH} + 0.559 \cdot \log_{10}[\text{F}^-] - 0.699 \cdot \log_{10}[\text{Cl}^-] \quad (\text{Eq. 4})$$

where the corrosion rate is in mm/yr, T is the absolute temperature in Kelvin, pH has its usual meaning, $[\text{F}^-]$ is the concentration of fluoride in parts per million, and $[\text{Cl}^-]$ is the concentration of chloride in parts per million. The squared correlation coefficient R^2 was 0.809. The signs of the coefficients for pH, $[\text{F}^-]$, and $[\text{Cl}^-]$ appear to be consistent with theory. They predict increasing corrosion rates with decreasing pH, decreasing chloride concentration, and increasing fluoride concentration. However, there is an apparent inconsistency as regards the temperature. The equation predicts that increasing the temperature will result in a decrease in the corrosion rate, which is inconsistent with theory and experience. Further, since the majority of the tests were performed at 55 °C or 80 °C, it is unreasonable to expect that the effect of temperature was well characterized.

A second fit was developed with the same data, but this time temperature was not included in the fit. The resulting correlation was:

$$\log_{10}(\text{corrosion rate}) = 1.51 - 0.661 \cdot \text{pH} + 0.678 \cdot \log_{10}[\text{F}^-] - 0.599 \cdot \log_{10}[\text{Cl}^-] \quad (\text{Eq. 5})$$

where the variables and units are as defined previously. The squared correlation coefficient R^2 for this correlation was 0.734.

To prepare the data for the linear least-squares fit, the software routine in Attachment I was used. The formulas shown in Attachment I were used to calculate the total fluoride and chloride concentration ($[\text{F}^-]$ and $[\text{Cl}^-]$, respectively), the inverse temperature ($1/T$), and the common logarithms of the total fluoride concentration, total chloride concentration, and corrosion rate ($\log_{10}[\text{F}^-]$, $\log_{10}[\text{Cl}^-]$, and $\log_{10}(\text{corrosion rate})$, respectively). As is discussed above, rows 9, 13, and 17 of the Excel spreadsheet listed in Attachment I were not included in

the fit. The molar masses used in stoichiometric calculations are from Lide (1995, inside front cover); these are accepted data because they are established fact.

The plot of the predicted versus actual corrosion rates is shown in Figure 11. It should be noted that the equation can be reduced to a simpler form if the Cl^-/F^- ratio is fixed, for example, the ratio of the chloride and fluoride ion concentrations quoted for J-13 well water. If this ratio is substituted into the last term of the equation, the corrosion rate is then dependent only on pH and fluoride content.

Using this approach, nominal values for each of the parameters were substituted into the equation to determine the pH values at which acceptably low corrosion rates would be predicted. The value obtained was in the pH 6-7 range, which is significantly higher than would be anticipated by theory. As noted earlier, this might be expected because no allowance was made in the empirical fit for the fact that there is a change in the chemical form at a pH of 3.18. It is, therefore, suggested that the above equation only be used to estimate corrosion rates at low pH values.

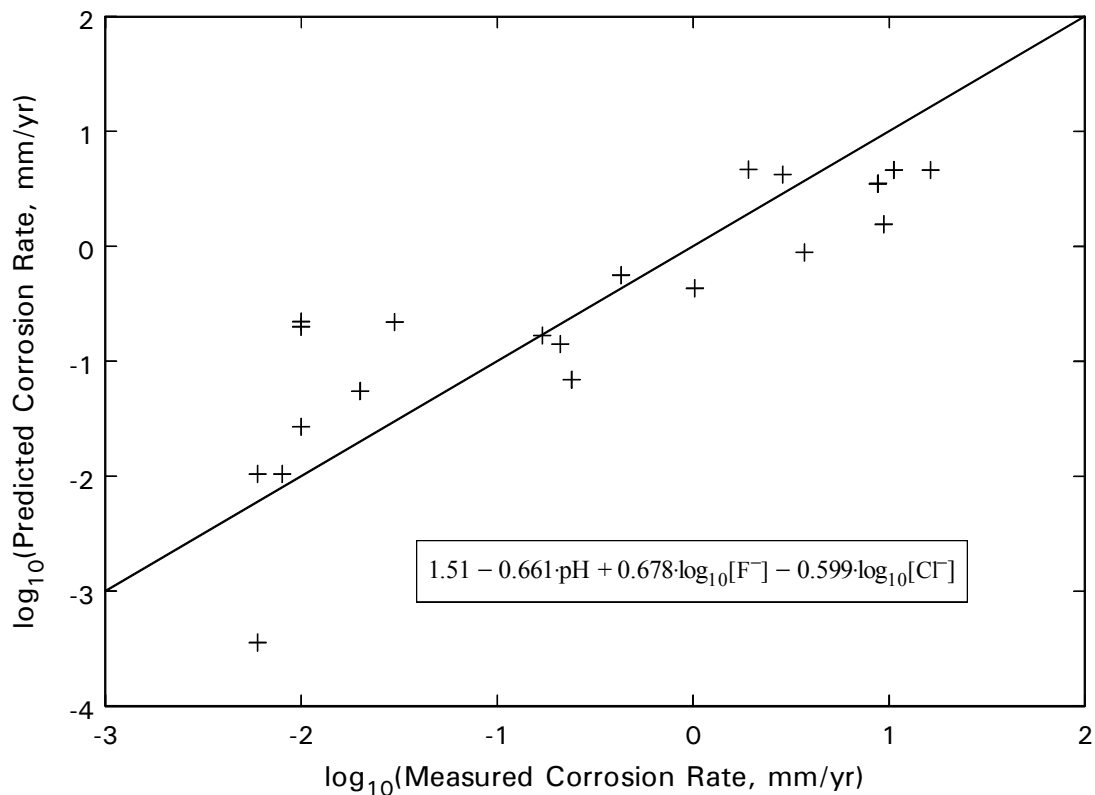


Figure 11. Predicted versus Measured Corrosion Rate as a Function of pH, F^- , and Cl^-

6.2.2.3.2 Theoretical Evaluation

Solutions with high fluoride contents do not necessarily cause accelerated corrosion. For accelerated corrosion to occur, the fluoride must be present as free ions, i.e., not complexed as compounds as discussed in Section 6.1.3, and the pH must be low. A high insoluble fluoride concentration, in essence a very low fluoride ion concentration, would not be expected to have much impact on the standard zirconium corrosion rate. Section 4.1.1 Test 12 shows that fluoride ion concentrations of less than 5 ppm, even at pH values as low as 1, produce similar corrosion rates to those with zero fluoride ion concentration. Thus, it is reasonable to conclude that low fluoride ion concentrations, as distinct from total fluoride content, will have limited impact on the uniform Zircaloy corrosion rate.

Zirconium and its alloys generally exhibit low corrosion rates in fluoride solutions, including relatively high fluoride ion content solutions, if the temperature is sufficiently low and the pH is sufficiently high. This is illustrated with the results in Section 4.1.1 Test 13. However, if the metal is in contact with solutions containing HF, the corrosion rate can increase rapidly. From the Pourbaix (1966) diagram shown in Figure 3, HF can exist when the pH is less than 3.18, although this does not necessarily mean that all fluoride ions are immediately converted to HF below this value. The data in Section 4.1.1 Tests 10 through 13 can be divided into fluoride ion-containing solutions and HF-containing solutions using a pH of 3.18 as the demarcation point. The highest corrosion rates obtained above and below the 3.18 value are summarized in Table 8. This assumes that calcium fluoride, due to its low solubility, does not contribute to the fluoride ion concentration, about 2 ppm at 25°C and less than 3 ppm at 90°C.

Table 8. A Simplified Set of Data Derived from Data in 4.1.1 Tests 10 to 13

Fluoride-containing Solution				HF-containing Solution			
F ⁻ , ppm	pH	°C	mm/yr	HF, ppm	pH	°C	mm/yr
100	7	100	0.008	0	0	80	0.01
5000	5	55	0.008	5	0	30	0.076
1000	5	55	0.006	20	0	30	0.127
1000	6.5	55	0.006	5	1	80	0.03
				20	1	80	0.43
				200	1	80	8.79
				200	3	80	0.17
				5000	1	55	16.3
				1000	1	55	10.6

It is evident from the table that HF containing solutions are highly corrosive when the pH is 1 and the HF concentration is greater than 5 ppm. The corrosion rate decreases significantly as the pH increases to 3. The rate decreases much further when the pH is 5 and HF, which is unstable at this pH, reverts to a fluoride ion solution. It will be noted that the corrosion rates for all the fluoride ion-containing solutions (fluoride ion concentrations between 100 and 5000 ppm, pH between 5 and 7 and temperature between 55°C and 100°C) are the same as the rate for zero fluoride/HF solutions at pH 0. This suggests that there is minimal effect of these high fluoride ion concentrations at high pH values and temperatures of 55°C or lower.

As discussed earlier, all of the above results were obtained on clean metal surfaces, i.e., with no post-transition oxide. By comparison, SNF cladding has a significant oxide thickness. The dissolution rate of such oxide in HF or fluoride ions is unknown, but the rate is unlikely to be faster than that of the alloy. Therefore, the observed values can be considered as worst case. Further, the experimental conditions used required that the fluoride ion concentration be constant throughout the test so that any fluoride depleted from the solutions by reaction with zirconium or its alloys were replenished as necessary. In practice this is unlikely to be the case. For example, if it is assumed that one liter of J-13 well water enters a waste package each year, the total contained fluorine content is 2.18 mg from Table 7. If it is further assumed that all the available fluorine reacts with zirconium to produce ZrF_4 , the maximum quantity of zirconium that could be corroded away is 2.64 mg per year ($4.04 \times 10^{-4} \text{ cm}^3/\text{year}$). This volume represents a cladding surface area of 0.008 square centimeters using a nominal wall thickness of 500 micron. This might be considered to be the worst possible hypothetical scenario. It would require the pH to decrease to a value below 3.18, ideally 1 or less, the fluoride content to concentrate significantly above 5 ppm, and all the water to concentrate in one spot on one fuel rod. Thus, assessments of fuel rod failures need to evaluate the total quantity of fluoride available for reaction in addition to the environmental conditions.

In summary, the following theoretical criteria are proposed for evaluation of the corrosion rate under HF/fluoride ion conditions.

- If the pH is maintained below 3.18 and the HF/fluoride ion concentration remains above 5 ppm, then the corrosion rate, weight loss, will be greater than 0.1 mm/year. At pH values in the 0 to 1 range and HF/fluoride concentrations in the 1000 to 5000 ppm range, the corrosion rate, weight loss, will be greater than 10 mm/year. These corrosion rates provide conservative estimates of the clad-life expectancy as a maximum of 5 years and feasibly as short as two weeks. They make no provision for other constraints such as the limited supply of fluoride ions as discussed above. This factor may, in fact, be the rate controlling criteria. For design purposes, it should be assumed that pH values below 3.18 will produce instantaneous cladding failure provided there is sufficient fluoride present to react with the cladding.
- If the pH is greater than 3.18 and the fluoride concentration is 5 ppm or less, then the corrosion rate, weight gain, will be in accordance with the Hillner et al. (1998) corrosion rate equation given in Section 6.2.1. (Eq. 2)
- If the pH is greater than 3.18, the fluoride concentration is greater than 5 ppm and the temperature is less than 55°C, then the corrosion rate is estimated between that calculated from the Hillner equation (weight gain) and 0.007 mm/year weight loss. The same assessment is made if the temperature is between 55 and 100°C and the fluoride concentration is 100 ppm or less. There is no data to provide corrosion rates at temperatures above 55°C and fluoride concentrations above 100 ppm. It should be noted that although no data is offered to support the recommendation for pH values between 3.18 and 5, it is reasonable to assume that the fluoride ion concentration controls the corrosion rate and the pH has no impact (Figure 3).

6.3 CORROSION CRITERIA AND ASSOCIATED RATES

For uniform corrosion, Hillner's equation is recommended as the best basis for calculating corrosion rates. Details are given in Section 6.2.1 (Eq. 2).

For accelerated corrosion and pitting to occur from the presence of ferric chloride, the conditions defined in Section 6.2.2.1 are required. If the solution pH remains above 2.5, the ferric ion is unstable and Hillner's corrosion equation rate can be used. Similarly, if the pH is below 2.5 and the local potential is less than 0.771 volts versus the NHE, ferric ions are not stable and Hillner's equation is acceptable. However, if conditions permit the presence of the ferric ion, the corrosion/pitting rates can be so fast that cladding can fail in very short times.

Sections 6.2.2.2 and 6.2.2.3 describe the conditions that could cause accelerated corrosion due to halides. An empirical correlation for calculating corrosion rates as a function of pH, fluoride and chloride ions has been developed but is only recommended for use at pH values below 3.18. A theoretical approach that defines the conditions under which various species can exist is considered more reliable for assessing accelerated corrosion at pH values above 3.18.

- If the pH is greater than 3.18 and the fluoride concentration is less than 5 ppm, then Hillner's equation can be used at any temperature.
- If the fluoride concentration is greater than 5 ppm and the temperature is less than 55°C or the fluoride concentration is less than 100 ppm and the temperature is between 55°C and 100°C, then the corrosion rate will vary between the weight gain predicted by the Hillner equation and a weight loss equivalent to 105 mg/dm² per year (7 micron/year). Insufficient data is currently available to define a better correlation.
- If the fluoride concentration is greater than 100 ppm and the temperature is greater than 55°C, then the corrosion rate can be so fast that cladding can fail in very short times.

No estimates are made of the percentage of rods that could be exposed to these failure modes and, thus, to the rod failure rates except to note that the controlling factor in Zircaloy cladding corrosion may be limited to the available quantity of the corroding media.

7. CONCLUSIONS

When subjected to oxygen-containing environments, zirconium and its alloys spontaneously form a layer of inert oxide film on exposed surfaces. This phenomenon is retained even in highly reducing environments such as hydrochloric acid and dilute sulfuric acid, where many passive alloys would otherwise not form protective oxide films. Zirconium alloys also provide excellent corrosion resistance in chloride-free oxidizing solutions such as nitric acid. Consequently, zirconium and its alloys have been used successfully for decades in many corrosive conditions in the chemical processing industry.

Additional points that can be made based on the information in this report include the following:

- All zirconium alloys are low in alloy content and are protected by a very adherent zirconium oxide film. Zirconium and its alloys have very similar corrosion resistance in a wide range of environments. However, they appear to exhibit a switch from excellent corrosion resistance to poor corrosion resistance over very narrow environmental bands. This phenomenon also differentiates the zirconium alloys. For example, the corrosion rate of all zirconium alloys is essentially the same in dilute sulfuric acid, but significant differences occur among alloys when the acid concentration is greater than 60%.
- The presence of fluorides in solutions can greatly degrade the corrosion resistance of zirconium and its alloys. Zirconium and its alloys have some resistance to fluoride corrosion only when the pH is high enough (greater than 3.18) and the temperature is low enough (less than 55°C). The criteria developed in Section 6.0 provide the conditions under which failure may occur. These conditions will be determined by the concentration and dilution of J-13 well water that contacts the cladding.
- Zirconium and its alloys resist localized corrosion such as pitting, crevice corrosion, and stress corrosion cracking, in all chloride solutions except the highly oxidizing chlorides. It has been noted that zirconium and its alloys are vulnerable to ferric chloride pitting, but this requires bulk pH values below 2.5. Above this value, the ferric ion does not exist. Corrosion will also not occur in crevices even when the pH is low since the condition is too reducing for the ferric ion to exist.

The equations and criteria recommended for evaluation of the corrosion rates follow.

For uniform corrosion of Zircaloy-2 and Zircaloy-4 under normal repository conditions:

$$\Delta\Delta W = 3.47 \times 10^7 \exp[-11452/T] \times \Delta t \quad (\text{Eq. 6})$$

where

$\Delta\Delta W$ is the weight gain in mg/dm^2 , Δt is the exposure time for corrosion in days, and T is the absolute temperature of the oxide/metal interfacial in Kelvin.

At a temperature of 100°C, the cladding will remain intact for at least 100,000 years. This relationship was obtained from data generated over 29 years and is considered very reliable.

For accelerated corrosion to occur by ferric chloride, the pH must be below 2.5, the local potential must exceed 0.771 volts versus normal hydrogen electrode, the ferric ion content must be above 50 ppm, the HCl concentration above 20%, and the temperature above 60°C. If these conditions exist, corrosion can be very rapid, and failure of the cladding can potentially occur in days or months.

For accelerated corrosion to occur in halide solutions in the absence of fluorides, the pH must be less than 1. When the pH is greater than 1, the passive film existing on the zirconium alloys has very low solubility and the corrosion rate may be considered to be that of uniform corrosion in water or steam.

For accelerated corrosion to occur in halide solutions containing fluorides, the following correlation was derived based on short-term corrosion data:

$$\text{Log}_{10}(\text{Corrosion rate}) = 1.51 - 0.661 \cdot \text{pH} + 0.678 \cdot \text{log}_{10}[\text{F}^-] - 0.599 \cdot \text{log}_{10}[\text{Cl}^-] \quad (\text{Eq. 7})$$

This correlation may be used for estimating corrosion rates when the pH is less than 3.18. It is not recommended for estimating corrosion rates at higher pH values.

The following theoretical approach is considered preferable for assessing corrosion rates in halide conditions:

- If the pH is maintained below 3.18 and the HF/fluoride ion concentration remains above 5 ppm, then the corrosion rate, weight loss, will be greater than 0.1 mm/year. At pH values in the 0 to 1 range and HF/fluoride concentrations in the 1000 to 5000 ppm range, the corrosion rate, weight loss, will be greater than 10 mm/year. These corrosion rates provide conservative estimates of the clad-life expectancy as a maximum of 5 years and feasibly as short as 2 weeks. They make no provision for other constraints such as the limited supply of fluoride ions as discussed above. This factor may, in fact, be the rate controlling criteria. For design purposes, it should be assumed that pH values below 3.18 will produce instantaneous cladding failure provided there is sufficient fluoride present to react with the cladding.
- If the pH is greater than 3.18 and the fluoride concentration is 5 ppm or less, then the corrosion rate, weight gain, will be in accordance with the Hillner corrosion rate equation given in Section 6.2.1.
- If the pH is greater than 3.18, the fluoride concentration is greater than 5 ppm, and the temperature is less than 55°C, then the corrosion rate is estimated to be between that calculated from the Hillner equation weight gain and 0.007 mm/year weight loss. The same assessment is made if the temperature is between 55 and 100°C and the fluoride concentration is 100 ppm or less. There is no data to provide corrosion rates at temperatures above 55°C and fluoride concentrations above 100 ppm. It should be noted that although no data is offered to support the recommendation for pH values between 3.18 and 5, it is reasonable to assume that the fluoride ion concentration controls the corrosion rate and the pH has no impact (Figure 3).

8. INPUTS AND REFERENCES

8.1 DOCUMENTS CITED

Andreeva, V.V. and Glukhova, A.I. 1961. "Corrosion and Electrochemical Properties of Zirconium, Titanium and Titanium-Zirconium Alloys in Solutions of Hydrochloric Acid and of Hydrochloric Acid with Oxidising Agents." *Journal of Applied Chemistry*, 11, 390-397. London, England: Society of Chemical Industry. TIC: 246101.

Andreeva, V.V. and Glukhova, A.I. 1962. "Corrosion and Electrochemical Properties of Titanium, Zirconium and Titanium-Zirconium Alloys in Acid Solutions. II." *Journal of Applied Chemistry*, 12, 457-468. London, England: Society of Chemical Industry. TIC: 246097.

Blumenthal, W.B. 1958. *The Chemical Behavior of Zirconium*. New York, New York: Van Nostrand. Library Tracking Number-L1402

Bradhurst, D.H. and Heuer, P.M. 1970. "The Influence of Oxide Stress on the Breakaway Oxidation of Zircaloy-2." *Journal of Nuclear Materials*, 37, 35-47. North- Holland, Amsterdam: North-Holland Publishing Company. TIC: 246048.

Brown, M.L. and Walton, G.N. 1975. "A Comparison of the Polarisation Behavior of Zirconium and its Alloys." *Journal of Nuclear Materials*, 58, (3), 321-335. Amsterdam, The Netherlands: North-Holland Publishing. TIC: 245897.

Burgers, W.G.; Claassen, A.; and Zernike, J. 1932. "Uber die chemische Natur der Oxydschichten, welche sich bei anodischer Polarisation auf den Metallen Aluminium, Zirkon, Titan und Tantal bilden." *Zeitschrift fur Physik*, 74, 593-603. Berlin, Germany: Springer-Verlag. TIC: 246091.

Charlesby, A. 1953. "Ionic Currents in Thin Films of Zirconium Oxide." *Acta Metallurgica*, 1, 340-347. New York, New York: Pergamon Press. TIC: 246056.

Cheng, B.C.; Kruger, R.M.; and Adamson, R.B. 1994. "Corrosion Behavior of Irradiated Zircaloy." *Zirconium in the Nuclear Industry, Tenth International Symposium, Baltimore, Maryland, June 21-24, 1993*. Garde, A.M. and Bradley, E.R., eds. *ASTM-STP-1245*, 400-418. Philadelphia, Pennsylvania: American Society for Testing and Materials. TIC: 246390.

Cox, B. 1970. "Factors Affecting the Growth of Porous Anodic Oxide Films on Zirconium." *Solid State Science Journal of the Electrochemical Society*, 117, (5), 654-663. New York, New York: Electrochemical Society. TIC: 246025.

Cragolino, G. and Galvele, J.R. 1978. "Anodic Behavior and Pitting of Zirconium and Zircaloy-4 in Aqueous Solutions of Sodium Chloride." *Passivity of Metals, Proceedings of the Fourth International Symposium on Passivity*. Frankenthal, R.P. and Kruger, J., eds. p. 1053-1057. Princeton, New Jersey: Electrochemical Society. TIC: 237155.

CRWMS M&O 1999. *1101213FM3 Waste Form Analyses & Models - PMR*. Activity Evaluation, December 14, 1999. Las Vegas, Nevada: CRWMS M&O. ACC: MOL.19991217.0048.

CRWMS M&O 1999. *Classification of the MGR Uncanistered Spent Nuclear Fuel Disposal Container System*. ANL-UDC-SE-000001 REV 00. Las Vegas, Nevada: CRWMS M&O. ACC: MOL.19990928.0216.

CRWMS M&O 2000. *Summary of In-Package Chemistry for Waste Forms*. ANL-EBS-MD-000050 REV 00. Las Vegas, Nevada: CRWMS M&O. ACC: MOL.20000217.0217.

CRWMS M&O 2000. *Waste Package Materials Department Analysis and Modeling Reports Supporting the Waste Form PMR*. TDP-EBS-MD-000005 REV 01 . Las Vegas, Nevada: CRWMS M&O. ACC: MOL.20000202.0173.

Dalgaard, S.B. 1962. "Corrosion and Hydriding Behaviour of Some Zr-2.5 wt.% Nb Alloys in Water, Steam and Various Gases at High Temperature." *Corrosion of Reactor Materials II, Proceedings of the Conference on Corrosion of Reactor Materials Held by the International Atomic Energy Agency at Europahaus, Salzburg, Austria, 4-8 June, 1962*. 159-191. Vienna, Austria: International Atomic Energy Agency. TIC: 247087.

DOE (U.S. Department of Energy) 2000. *Quality Assurance Requirements and Description*. DOE/RW-0333P, Rev. 9. Washington, D.C.: U.S. Department of Energy, Office of Civilian Radioactive Waste Management. ACC: MOL.19991028.0012.

Etherington, H.; Dalzell, R.C.; Lillie, D.W. 1955. "Zirconium and its Application to Nuclear Reactors." *The Metallurgy of Zirconium, 1st Edition*. Lustman, B.; Kerze, F., Jr. New York, New York: McGraw-Hill. TIC: 246326.

Etoh, Y.; Kikuchi, K.; Yasuda, T.; Koizumi, S.; and Oishi, M. 1991. "Neutron Irradiation Effects on the Nodular Corrosion of Zircaloy-2." *Fuel for the 90's: Proceedings, International Topical Meeting on LWR Fuel Performance, Avignon, France, April 21-24, 1991. Volume 2*, 691-700. La Grange Park, Illinois: American Nuclear Society. TIC: 243519.

Etoh, Y.; Shimada, S.; Kikuchi, K.; and Kawai, K. 1992. "Irradiation Effects on Corrosion Resistance and Microstructure of Zircaloy-4." *Journal of Nuclear Science and Technology*, 29, (12), 1173-1183. Tokyo, Japan: Atomic Energy Society of Japan. TIC: 246085.

Fahey, J.; Holmes, D.; and Yau, T.-L. 1997. "Evaluation of Localized Corrosion of Zirconium in Acidic Chloride Solutions." *Corrosion*, 53, (1), 54-61. Houston, Texas: National Association of Corrosion Engineers. TIC: 238103.

Fitzgerald, B.J. and Yau, T. 1993. "The Mechanism and Control of Stress Corrosion Cracking of Zirconium in Sulfuric Acid." *Corrosion Control for Low-Cost Reliability, 12th International Corrosion Congress, Houston, Texas, September 19-24, 1993*, 2, 762-777. Houston, Texas: National Association of Corrosion Engineers. Library Tracking Number-L1403

Fontana, M.G. 1986. *Corrosion Engineering*. 3rd Edition. New York, New York: McGraw-Hill. TIC: 240700.

Godlewski, J. 1994. "How the Tetragonal Zirconia is Stabilized in the Oxide Scale that is Formed on a Zirconium Alloy Corroded at 400(Degree)C in Steam." *Zirconium in the Nuclear Industry: Tenth International Symposium. ASTM STP 1245*, 679. Philadelphia, Pennsylvania: American Society for Testing and Materials. TIC: 246390.

Godlewski, J.; Gros, J.P.; Lambertin, M.; Wadier, J.F.; and Weidinger, H. 1991. "Raman Spectroscopy Study of the Tetragonal-to-Monoclinic Transition in Zirconium Oxide Scales and Determination of Overall Oxygen Diffusion by Nuclear Microanalysis of O18." *Zirconium in the Nuclear Industry, Ninth International Symposium, Kobe, Japan, November 5-8, 1990*. Eucken, C.M. and Garde, A.M., eds. *ASTM STP 1132*, 416-433. Philadelphia, Pennsylvania: American Society for Testing and Materials. TIC: 246113.

Hillner, E.; Franklin, D.G.; and Smee, J.D. 1998. *The Corrosion of Zircaloy-Clad Fuel Assemblies in a Geologic Repository Environment*. WAPD-T-3173. West Mifflin, Pennsylvania: Bettis Atomic Power Laboratory. TIC: 237127.

Holzer, R. and Stehle, H. 1986. "Development in Design and Engineering of KWU Fuel for Light and Heavy Water Reactors." *Conference Proceedings: International Conference on CANDU Fuel*. 26, 28. Chalk River, Ontario, Canada: Atomic Energy of Canada Limited. Library Tracking Number-L0975

Jangg, V.G.; Webster, R.T.; and Simon, J.M. 1978. "Untersuchung uber das Korrosionsverhalten von Zirkoniumlegierungen." *Werkstoffe und Korrosion*, 29, 16-26. Weinheim, Germany: VCH Gesellschaft GmbH. TIC: 246090.

Kass, S. 1964. "The Development of the Zircalloys." *Corrosion of Zirconium Alloys, A Symposium Presented at the 1963 Winter Meeting, American Nuclear Society, New York, N.Y., November 20, 1963*. ASTM Special Technical Publication No. 368. Pages 3-27. Philadelphia, Pennsylvania: American Society for Testing and Materials. TIC: 247110.

Khatamian, D. and Lalonde, S.D. 1997. "Crystal Structure of Thin Oxide Films Grown on Zr-Nb Alloys Studied by RHEED." *Journal of Nuclear Materials*, 245, 10-16. Amsterdam, The Netherlands: Elsevier Science B.V. TIC: 246039.

Latimer, W.M. 1952. *The Oxidation States of the Elements and Their Oxidation Potentials in Aqueous Solutions*. Pages 8, 9, 30, 215, 270, 271, 272, 273 and 274. New York, New York: Prentice-Hall. TIC: 238748.

Lide, D.R., ed. 1995. *CRC Handbook of Chemistry and Physics*. 76th Edition. Boca Raton, Florida: CRC Press. TIC: 216194.

Lustman, B. and Kerze, F., Jr. 1955. *The Metallurgy of Zirconium*. 1st Edition. New York, New York: McGraw-Hill Book Company. TIC: 246326.

Maguire, M. 1984. "The Pitting Susceptibility of Zirconium in Aqueous Cl-, Br-, and I-Solutions." *Industrial Applications of Titanium and Zirconium: Third Conference, A Symposium Sponsored by ASTM Committee B-10 on Reactive and Refractory Metals and Alloys, New Orleans, Louisiana, September 21-23, 1982. ASTM STP 830*, p. 177-189. Philadelphia, Pennsylvania: American Society for Testing and Materials. TIC: 237161.

Maraghini, M.; Adams, G.B., Jr.; and Van Rysselberge, P. 1954. "Studies on the Anodic Polarization of Zirconium and Zirconium Alloys." *Journal of the Electrochemical Society*, 101, (8), 400-408. New York, New York: Electrochemical Society. TIC: 245950.

Pourbaix, M. 1966. *Atlas of Electrochemical Equilibria in Aqueous Solutions*. Long Island City, New York: Pergamon Press. TIC: 240774.

Roy, C. and David, G. 1970. "X-ray Diffraction Analyses of Zirconia Films on Zirconium and Zircaloy-2." *Journal of Nuclear Materials*, 37, (1), 71-81. Amsterdam, The Netherlands: North-Holland Publishing Company. TIC: 246047.

Shibata, T. and Ameer, M.A.M. 1992. "Stochastic Processes of Pit Generation on Zirconium With an Anodic Oxide Film." *Corrosion Science*, 33, (10), 1633-1643. New York, New York: Pergamon Press. TIC: 245949.

Shunk, F.A. 1969. *Constitution of Binary Alloys*. Second Supplement. New York, New York: McGraw-Hill Book Company. Library Tracking Number-L1404

Stehle, H.; Garzarolli, F.; Garde, A.M.; and Smerde, P.G. 1984. "Characterization of ZrO₂ Films Formed In-Reactor and Ex-Reactor to Study the Factors Contributing to the In-Reactor Waterside Corrosion of Zircaloy." *Zirconium in the Nuclear Industry, Sixth International Symposium, Vancouver, British Columbia, June 28- July 1, 1982*. Franklin, D.G. and Adamson, R.B., eds. *ASTM STP 824*, 483-505. Philadelphia, Pennsylvania: American Society for Testing and Materials. TIC: 241417.

Thomas, D.E. 1955. "Corrosion in Water and Steam." *The Metallurgy of Zirconium*. Lustman, B. and Kerze, F., Jr. 1st Edition. New York, New York: McGraw-Hill. TIC: 246326.

Uziemblo, N.H. and Smith, H.D. 1989. *An Investigation of the Influence of Fluoride on the Corrosion of Zircaloy-4: Initial Report*. PNL-6859. Draft. Richland, Washington: Pacific Northwest Laboratory. ACC: MOL.19980326.0369.

Whitton, J.L. 1968. "The Measurement of Ionic Mobilities in the Anodic Oxides of Tantalum and Zirconium by a Precision Sectioning Technique." *Journal of the Electrochemical Society*, 115, (1), 58-61. Pennington, New Jersey: Electrochemical Society. TIC: 245895.

Yau, T-L. 1983. "Performance of Zirconium and Columbium in Simulated FGD Scrubber Solutions." *Corrosion 83, International Corrosion Forum, Anaheim, California, April 18-22, 1983*. Pages 191/1-191/11. Houston, Texas: National Association of Corrosion Engineers. TIC: 247246.

Yau, T.-L. 1992. "Stress-Corrosion Cracking of Zirconium Alloys." 11 *Stress-Corrosion Cracking*. Jones, R.H. 299-311. Materials Park, Ohio: ASM International. TIC: 246059.

Yau, T.L. and Maguire, M. 1990. "Control of Localized Corrosion of Zirconium in Oxidizing Chloride Media." *Advances in Localized Corrosion, Proceedings of the Second International Conference on Localized Corrosion, June 1-5, 1987, Orlando, Florida*. Isaacs, H.S.; Bertocci, U.; Kruger, J. and Smialowska, S., eds. Pages 311-319. Houston, Texas: National Association of Corrosion Engineers. TIC: 247083.

Yau, T.L. and Webster, R.T. 1987. "Corrosion of Zirconium and Hafnium." *ASM Handbook (Formerly Ninth Edition, Metals Handbook), Volume 13, Corrosion*. p. 707-721. Materials Park, Ohio: American Society for Metals. TIC: 240704.

8.2 CODES, STANDARDS, REGULATIONS, AND PROCEDURES

AP-3.10Q, Rev. 2, ICN 0. *Analyses and Models*. Washington, D.C.: U.S. Department of Energy, Office of Civilian Radioactive Waste Management. ACC: MOL.20000217.0246.

ASTM STP 639. 1977. *Manual on Zirconium and Hafnium*. Philadelphia, Pennsylvania: American Society for Testing and Materials. TIC: 246398.

QAP-2-3, Rev. 10. *Classification of Permanent Items*. Las Vegas, Nevada: CRWMS M&O. ACC: MOL.19990316.0006.

QAP-2-0, Rev. 5, ICN 1. *Conduct of Activities*. Las Vegas, Nevada: CRWMS M&O. ACC: MOL.19991109.0221.

ATTACHMENTS

Attachment	Title
I.	Equations 4 and 5 Software Routine
II.	Industrial Applications of Zirconium and Its Alloys
III.	Zircaloy Metallurgy

"zirc_corr_rate3.xls" Software Routine Used to Develop Equations 4 and 5

	A	B	C	D	E	F	G	H	I	J	K	L	M	N	O	P	Q
1	Line	Corrosion	Temp	CaCl ₂	MgCl ₂	NaF (F ⁻)	CaF ₂ (F ⁻)	pH	NaCl	KCl	F ⁻	Cl ⁻					
2	No.	mm/yr	K	ppm	ppm	ppm	ppm		ppm	ppm	ppm	ppm	Inv. T	pH	log ₁₀ [F ⁻]	log ₁₀ [Cl ⁻]	log ₁₀ (corr)
3	1	0.03	353	2000	1000	5	0	1			=F3+G3	=D3*2*mCl/(mCa+2*mCl)+E3*2*mCl/(mMg+2*mCl)+I3*mCl/(mNa+mCl)+J3*mCl/(mK+mCl)	=1/C3	=H3	=LOG(K3)	=LOG(L3)	=LOG(B3)
4	2	0.43	353	2000	1000	20	0	1			=F4+G4	=D4*2*mCl/(mCa+2*mCl)+E4*2*mCl/(mMg+2*mCl)+I4*mCl/(mNa+mCl)+J4*mCl/(mK+mCl)	=1/C4	=H4	=LOG(K4)	=LOG(L4)	=LOG(B4)
5	3	0.02	353	20000	10000	5	0	1			=F5+G5	=D5*2*mCl/(mCa+2*mCl)+E5*2*mCl/(mMg+2*mCl)+I5*mCl/(mNa+mCl)+J5*mCl/(mK+mCl)	=1/C5	=H5	=LOG(K5)	=LOG(L5)	=LOG(B5)
6	4	0.21	353	20000	10000	20	0	1			=F6+G6	=D6*2*mCl/(mCa+2*mCl)+E6*2*mCl/(mMg+2*mCl)+I6*mCl/(mNa+mCl)+J6*mCl/(mK+mCl)	=1/C6	=H6	=LOG(K6)	=LOG(L6)	=LOG(B6)
7	5	0.01	353	66000	33000	5	0	1			=F7+G7	=D7*2*mCl/(mCa+2*mCl)+E7*2*mCl/(mMg+2*mCl)+I7*mCl/(mNa+mCl)+J7*mCl/(mK+mCl)	=1/C7	=H7	=LOG(K7)	=LOG(L7)	=LOG(B7)
8	6	0.24	353	66000	33000	20	0	1			=F8+G8	=D8*2*mCl/(mCa+2*mCl)+E8*2*mCl/(mMg+2*mCl)+I8*mCl/(mNa+mCl)+J8*mCl/(mK+mCl)	=1/C8	=H8	=LOG(K8)	=LOG(L8)	=LOG(B8)
9	7	0.01	353	2000	1000	0	0	1			=F9+G9	=D9*2*mCl/(mCa+2*mCl)+E9*2*mCl/(mMg+2*mCl)+I9*mCl/(mNa+mCl)+J9*mCl/(mK+mCl)	=1/C9	=H9	=LOG(K9)	=LOG(L9)	=LOG(B9)
10	8	8.79	353	2000	1000	200	100	1			=F10+G10	=D10*2*mCl/(mCa+2*mCl)+E10*2*mCl/(mMg+2*mCl)+I10*mCl/(mNa+mCl)+J10*mCl/(mK+mCl)	=1/C10	=H10	=LOG(K10)	=LOG(L10)	=LOG(B10)
11	9	8.79	353	2000	1000	0	300	1			=F11+G11	=D11*2*mCl/(mCa+2*mCl)+E11*2*mCl/(mMg+2*mCl)+I11*mCl/(mNa+mCl)+J11*mCl/(mK+mCl)	=1/C11	=H11	=LOG(K11)	=LOG(L11)	=LOG(B11)
12	10	0.17	353	2000	1000	200	100	3			=F12+G12	=D12*2*mCl/(mCa+2*mCl)+E12*2*mCl/(mMg+2*mCl)+I12*mCl/(mNa+mCl)+J12*mCl/(mK+mCl)	=1/C12	=H12	=LOG(K12)	=LOG(L12)	=LOG(B12)
13	11	0	353	20000	10000	0	0	1			=F13+G13	=D13*2*mCl/(mCa+2*mCl)+E13*2*mCl/(mMg+2*mCl)+I13*mCl/(mNa+mCl)+J13*mCl/(mK+mCl)	=1/C13	=H13	=LOG(K13)	=LOG(L13)	=LOG(B13)
14	12	2.87	353	20000	10000	200	2800	1			=F14+G14	=D14*2*mCl/(mCa+2*mCl)+E14*2*mCl/(mMg+2*mCl)+I14*mCl/(mNa+mCl)+J14*mCl/(mK+mCl)	=1/C14	=H14	=LOG(K14)	=LOG(L14)	=LOG(B14)
15	13	3.71	353	20000	10000	0	300	1			=F15+G15	=D15*2*mCl/(mCa+2*mCl)+E15*2*mCl/(mMg+2*mCl)+I15*mCl/(mNa+mCl)+J15*mCl/(mK+mCl)	=1/C15	=H15	=LOG(K15)	=LOG(L15)	=LOG(B15)
16	14	0.01	353	20000	10000	200	2800	3			=F16+G16	=D16*2*mCl/(mCa+2*mCl)+E16*2*mCl/(mMg+2*mCl)+I16*mCl/(mNa+mCl)+J16*mCl/(mK+mCl)	=1/C16	=H16	=LOG(K16)	=LOG(L16)	=LOG(B16)
17	15	0.01	353	66000	33000	0	0	1			=F17+G17	=D17*2*mCl/(mCa+2*mCl)+E17*2*mCl/(mMg+2*mCl)+I17*mCl/(mNa+mCl)+J17*mCl/(mK+mCl)	=1/C17	=H17	=LOG(K17)	=LOG(L17)	=LOG(B17)
18	16	1.92	353	66000	33000	200	9800	1			=F18+G18	=D18*2*mCl/(mCa+2*mCl)+E18*2*mCl/(mMg+2*mCl)+I18*mCl/(mNa+mCl)+J18*mCl/(mK+mCl)	=1/C18	=H18	=LOG(K18)	=LOG(L18)	=LOG(B18)
19	17	1.02	353	66000	33000	0	300	1			=F19+G19	=D19*2*mCl/(mCa+2*mCl)+E19*2*mCl/(mMg+2*mCl)+I19*mCl/(mNa+mCl)+J19*mCl/(mK+mCl)	=1/C19	=H19	=LOG(K19)	=LOG(L19)	=LOG(B19)
20	18	0.01	353	66000	33000	200	9800	3			=F20+G20	=D20*2*mCl/(mCa+2*mCl)+E20*2*mCl/(mMg+2*mCl)+I20*mCl/(mNa+mCl)+J20*mCl/(mK+mCl)	=1/C20	=H20	=LOG(K20)	=LOG(L20)	=LOG(B20)
21	19	16.3	328	15000	10000	5000	0	1	15000	10000	=F21+G21	=D21*2*mCl/(mCa+2*mCl)+E21*2*mCl/(mMg+2*mCl)+I21*mCl/(mNa+mCl)+J21*mCl/(mK+mCl)	=1/C21	=H21	=LOG(K21)	=LOG(L21)	=LOG(B21)
22	20	0.008	328	15000	10000	5000	0	5	15000	10000	=F22+G22	=D22*2*mCl/(mCa+2*mCl)+E22*2*mCl/(mMg+2*mCl)+I22*mCl/(mNa+mCl)+J22*mCl/(mK+mCl)	=1/C22	=H22	=LOG(K22)	=LOG(L22)	=LOG(B22)
23	21	0.006	328	15000	10000	1000	4000	5	15000	10000	=F23+G23	=D23*2*mCl/(mCa+2*mCl)+E23*2*mCl/(mMg+2*mCl)+I23*mCl/(mNa+mCl)+J23*mCl/(mK+mCl)	=1/C23	=H23	=LOG(K23)	=LOG(L23)	=LOG(B23)
24	22	10.6	328	15000	10000	1000	4000	1	15000	10000	=F24+G24	=D24*2*mCl/(mCa+2*mCl)+E24*2*mCl/(mMg+2*mCl)+I24*mCl/(mNa+mCl)+J24*mCl/(mK+mCl)	=1/C24	=H24	=LOG(K24)	=LOG(L24)	=LOG(B24)
25	23	0.006	328	15000	10000	1000	0	6.5	15000	10000	=F25+G25	=D25*2*mCl/(mCa+2*mCl)+E25*2*mCl/(mMg+2*mCl)+I25*mCl/(mNa+mCl)+J25*mCl/(mK+mCl)	=1/C25	=H25	=LOG(K25)	=LOG(L25)	=LOG(B25)
26	24	9.4	328	15000	10000	1000	0	1	15000	10000	=F26+G26	=D26*2*mCl/(mCa+2*mCl)+E26*2*mCl/(mMg+2*mCl)+I26*mCl/(mNa+mCl)+J26*mCl/(mK+mCl)	=1/C26	=H26	=LOG(K26)	=LOG(L26)	=LOG(B26)
27																	
28		Molar															
29		masses	g/mol														
30		mNa	22.989768														
31		mMg	24.305														
32		mCl	35.4527														
33		mK	39.0983														
34		mCa	40.078														
35																	
36																	
37																	

Cells A3..A26 (Line No.) do not contain data; they are for traceability only.

Cells B3..J26 contain data from Tables 4-1, 4-2.

Cells K3..Q26 contain calculated results. "F" ppm respectively, in ppm. "Inv. T" is the inverse of the and "log₁₀(corr)" are the common logarithms of the corrosion rate as reported in columns K, L, and B.

Cells C30..C34 contain molar masses from Lide

The name for cell C30 (mNa) is in cell B30; the first letter of each name ("m") indicates "molar"

"zirc_corr_rate3.xls" Software Routine Used to Develop Equations 4 and 5

	A	B	C	D	E	F	G	H	I	J	K
1	Line	Corrosion	Temp	CaCl ₂	MgCl ₂	NaF (F ⁻)	CaF ₂ (F ⁻)	pH	NaCl	KCl	F ⁻
2	No.	mm/yr	K	ppm	ppm	ppm	ppm		ppm	ppm	ppm
3	1	0.03	353	2000	1000	5	0	1			=F3+G3
4	2	0.43	353	2000	1000	20	0	1			=F4+G4
5	3	0.02	353	20000	10000	5	0	1			=F5+G5
6	4	0.21	353	20000	10000	20	0	1			=F6+G6
7	5	0.01	353	66000	33000	5	0	1			=F7+G7
8	6	0.24	353	66000	33000	20	0	1			=F8+G8
9	7	0.01	353	2000	1000	0	0	1			=F9+G9
10	8	8.79	353	2000	1000	200	100	1			=F10+G10
11	9	8.79	353	2000	1000	0	300	1			=F11+G11
12	10	0.17	353	2000	1000	200	100	3			=F12+G12
13	11	0	353	20000	10000	0	0	1			=F13+G13
14	12	2.87	353	20000	10000	200	2800	1			=F14+G14
15	13	3.71	353	20000	10000	0	300	1			=F15+G15
16	14	0.01	353	20000	10000	200	2800	3			=F16+G16
17	15	0.01	353	66000	33000	0	0	1			=F17+G17
18	16	1.92	353	66000	33000	200	9800	1			=F18+G18
19	17	1.02	353	66000	33000	0	300	1			=F19+G19
20	18	0.01	353	66000	33000	200	9800	3			=F20+G20
21	19	16.3	328	15000	10000	5000	0	1	15000	10000	=F21+G21
22	20	0.008	328	15000	10000	5000	0	5	15000	10000	=F22+G22
23	21	0.006	328	15000	10000	1000	4000	5	15000	10000	=F23+G23
24	22	10.6	328	15000	10000	1000	4000	1	15000	10000	=F24+G24
25	23	0.006	328	15000	10000	1000	0	6.5	15000	10000	=F25+G25
26	24	9.4	328	15000	10000	1000	0	1	15000	10000	=F26+G26
27											
28		Molar									Cells A3..A26 (Line No.) do not contain data; they are for traceability only.
29		masses	g/mol								Cells B3..J26 contain data from Tables 4-1, 4-2,
30		mNa	22.989768								Cells K3..Q26 contain calculated results. "F ⁻ ppm"
31		mMg	24.305								respectively, in ppm. "Inv. T" is the inverse of the
32		mCl	35.4527								and "log ₁₀ (corr)" are the common logarithms of the
33		mK	39.0983								corrosion rate as reported in columns K, L, and B,
34		mCa	40.078								Cells C30..C34 contain molar masses from Lide
35											The name for cell C30 (mNa) is in cell B30; the
36											The first letter of each name ("m") indicates "molar

"zirc_corr_rate3.xls" Software Routine Used to Develop Equations 4 and 5

	L	M	N	O	P	Q
1	Cl ⁻					
2	ppm	Inv. T	pH	log ₁₀ [F]	log ₁₀ [Cl]	log ₁₀ (corr)
3	=D3*2*mCl/(mCa+2*mCl)+E3*2*mCl/(mMg+2*mCl)+I3*mCl/(mNa+mCl)+J3*mCl/(mK+mCl)	=1/C3	=H3	=LOG(K3)	=LOG(L3)	=LOG(B3)
4	=D4*2*mCl/(mCa+2*mCl)+E4*2*mCl/(mMg+2*mCl)+I4*mCl/(mNa+mCl)+J4*mCl/(mK+mCl)	=1/C4	=H4	=LOG(K4)	=LOG(L4)	=LOG(B4)
5	=D5*2*mCl/(mCa+2*mCl)+E5*2*mCl/(mMg+2*mCl)+I5*mCl/(mNa+mCl)+J5*mCl/(mK+mCl)	=1/C5	=H5	=LOG(K5)	=LOG(L5)	=LOG(B5)
6	=D6*2*mCl/(mCa+2*mCl)+E6*2*mCl/(mMg+2*mCl)+I6*mCl/(mNa+mCl)+J6*mCl/(mK+mCl)	=1/C6	=H6	=LOG(K6)	=LOG(L6)	=LOG(B6)
7	=D7*2*mCl/(mCa+2*mCl)+E7*2*mCl/(mMg+2*mCl)+I7*mCl/(mNa+mCl)+J7*mCl/(mK+mCl)	=1/C7	=H7	=LOG(K7)	=LOG(L7)	=LOG(B7)
8	=D8*2*mCl/(mCa+2*mCl)+E8*2*mCl/(mMg+2*mCl)+I8*mCl/(mNa+mCl)+J8*mCl/(mK+mCl)	=1/C8	=H8	=LOG(K8)	=LOG(L8)	=LOG(B8)
9	=D9*2*mCl/(mCa+2*mCl)+E9*2*mCl/(mMg+2*mCl)+I9*mCl/(mNa+mCl)+J9*mCl/(mK+mCl)	=1/C9	=H9	=LOG(K9)	=LOG(L9)	=LOG(B9)
10	=D10*2*mCl/(mCa+2*mCl)+E10*2*mCl/(mMg+2*mCl)+I10*mCl/(mNa+mCl)+J10*mCl/(mK+mCl)	=1/C10	=H10	=LOG(K10)	=LOG(L10)	=LOG(B10)
11	=D11*2*mCl/(mCa+2*mCl)+E11*2*mCl/(mMg+2*mCl)+I11*mCl/(mNa+mCl)+J11*mCl/(mK+mCl)	=1/C11	=H11	=LOG(K11)	=LOG(L11)	=LOG(B11)
12	=D12*2*mCl/(mCa+2*mCl)+E12*2*mCl/(mMg+2*mCl)+I12*mCl/(mNa+mCl)+J12*mCl/(mK+mCl)	=1/C12	=H12	=LOG(K12)	=LOG(L12)	=LOG(B12)
13	=D13*2*mCl/(mCa+2*mCl)+E13*2*mCl/(mMg+2*mCl)+I13*mCl/(mNa+mCl)+J13*mCl/(mK+mCl)	=1/C13	=H13	=LOG(K13)	=LOG(L13)	=LOG(B13)
14	=D14*2*mCl/(mCa+2*mCl)+E14*2*mCl/(mMg+2*mCl)+I14*mCl/(mNa+mCl)+J14*mCl/(mK+mCl)	=1/C14	=H14	=LOG(K14)	=LOG(L14)	=LOG(B14)
15	=D15*2*mCl/(mCa+2*mCl)+E15*2*mCl/(mMg+2*mCl)+I15*mCl/(mNa+mCl)+J15*mCl/(mK+mCl)	=1/C15	=H15	=LOG(K15)	=LOG(L15)	=LOG(B15)
16	=D16*2*mCl/(mCa+2*mCl)+E16*2*mCl/(mMg+2*mCl)+I16*mCl/(mNa+mCl)+J16*mCl/(mK+mCl)	=1/C16	=H16	=LOG(K16)	=LOG(L16)	=LOG(B16)
17	=D17*2*mCl/(mCa+2*mCl)+E17*2*mCl/(mMg+2*mCl)+I17*mCl/(mNa+mCl)+J17*mCl/(mK+mCl)	=1/C17	=H17	=LOG(K17)	=LOG(L17)	=LOG(B17)
18	=D18*2*mCl/(mCa+2*mCl)+E18*2*mCl/(mMg+2*mCl)+I18*mCl/(mNa+mCl)+J18*mCl/(mK+mCl)	=1/C18	=H18	=LOG(K18)	=LOG(L18)	=LOG(B18)
19	=D19*2*mCl/(mCa+2*mCl)+E19*2*mCl/(mMg+2*mCl)+I19*mCl/(mNa+mCl)+J19*mCl/(mK+mCl)	=1/C19	=H19	=LOG(K19)	=LOG(L19)	=LOG(B19)
20	=D20*2*mCl/(mCa+2*mCl)+E20*2*mCl/(mMg+2*mCl)+I20*mCl/(mNa+mCl)+J20*mCl/(mK+mCl)	=1/C20	=H20	=LOG(K20)	=LOG(L20)	=LOG(B20)
21	=D21*2*mCl/(mCa+2*mCl)+E21*2*mCl/(mMg+2*mCl)+I21*mCl/(mNa+mCl)+J21*mCl/(mK+mCl)	=1/C21	=H21	=LOG(K21)	=LOG(L21)	=LOG(B21)
22	=D22*2*mCl/(mCa+2*mCl)+E22*2*mCl/(mMg+2*mCl)+I22*mCl/(mNa+mCl)+J22*mCl/(mK+mCl)	=1/C22	=H22	=LOG(K22)	=LOG(L22)	=LOG(B22)
23	=D23*2*mCl/(mCa+2*mCl)+E23*2*mCl/(mMg+2*mCl)+I23*mCl/(mNa+mCl)+J23*mCl/(mK+mCl)	=1/C23	=H23	=LOG(K23)	=LOG(L23)	=LOG(B23)
24	=D24*2*mCl/(mCa+2*mCl)+E24*2*mCl/(mMg+2*mCl)+I24*mCl/(mNa+mCl)+J24*mCl/(mK+mCl)	=1/C24	=H24	=LOG(K24)	=LOG(L24)	=LOG(B24)
25	=D25*2*mCl/(mCa+2*mCl)+E25*2*mCl/(mMg+2*mCl)+I25*mCl/(mNa+mCl)+J25*mCl/(mK+mCl)	=1/C25	=H25	=LOG(K25)	=LOG(L25)	=LOG(B25)
26	=D26*2*mCl/(mCa+2*mCl)+E26*2*mCl/(mMg+2*mCl)+I26*mCl/(mNa+mCl)+J26*mCl/(mK+mCl)	=1/C26	=H26	=LOG(K26)	=LOG(L26)	=LOG(B26)
27						
28						
29						
30						
31						
32						
33						
34						
35						
36						

ATTACHMENT II

INDUSTRIAL APPLICATIONS OF ZIRCONIUM AND ITS ALLOYS

This attachment provides a brief description of the use of zirconium and its alloys in a variety of industrial applications. The purpose of providing this information is to demonstrate the superior corrosion resistance of zirconium compared to stainless steel, graphite, titanium, nickel alloys, and other highly corrosion resistant materials in a variety of adverse chemical conditions.

Zirconium and its alloys have been used in the CPI for more than 40 years as structural materials in fabricating columns, reactors, heat exchangers, vaporizers, pumps, piping systems, valves, and agitators. Zirconium's ability to solve a variety of corrosion problems was recognized at an early stage, particularly in HCl applications, which are among the most corrosive applications to handle. The following provides information on uses in HCl applications and other corrosive environments including sulfuric acid, nitric acid, peroxide, and halides.

II.1 UREA

Zirconium is used in the production of urea where vessels and heat exchangers have shown no signs of corrosion after more than thirty years in service.

The most corrosive chemical in this process is ammonium carbamate. To achieve high conversion rates, the process operates at elevated temperatures and pressures, and these conditions are too corrosive for stainless alloys.

II.2 ACETIC ACID

Zirconium is an important component in the manufacture of acetic acid. A modern plant can use more than 100 tons of zirconium.

The current process utilizes the reaction between methanol and carbon monoxide. The reaction proceeds at high temperature (150°C or greater) and high-pressure (3.3 to 6.6 MPa) in the presence of a halide catalyst, typically an iodide. For corrosion resistance, much of the process equipment is manufactured from Zr 702 and Zr 705 because the operating conditions would induce excessive corrosion in stainless alloys, due to the following:

- The intermediate acid concentration
- The high temperature
- The highly corrosive nature of methanol and iodides.

II.3 FORMIC ACID

Zirconium is used as the structural material for the main equipment in the production of formic acid by the hydrolysis of methyl formate.

Formic acid is more highly ionized and, therefore, more corrosive than acetic acid. Stainless steels can be seriously attacked by intermediate strengths of hot formic acid. Similarly nickel-based alloys and titanium do not perform well under formic acid process conditions. The elevated temperatures and pressures used in the process and the presence of water and catalyst make other corrosion resistant materials, including glass lining and resin and plastic coatings, inadequate as structural materials for this process.

II.4 PEROXIDE AND OTHER SULFURIC ACID-CONTAINING PROCESSES

Zirconium is preferred over graphite for the production of hydrogen peroxide by the electrolysis of acid sulfates. Although the process is extremely corrosive, peroxide strengths of 90% are now produced with zirconium equipment. The average maintenance-free life of the heat exchanger has increased to ten years using zirconium compared to a typical service life of twelve to eighteen months using graphite components. The sulfuric acid strength in this application is typically 35% H₂SO₄.

Based on the peroxide production experience, zirconium is now replacing graphite heat exchangers in the manufacture of acrylic films and fibers. In this application, the H₂SO₄ concentration can be as high as 60% at 150°C. Similarly, zirconium is widely used in the manufacture of butyl alcohol. These conditions require 60 to 65% H₂SO₄ at temperatures slightly above boiling.

Other organic production processes in which zirconium has found favor and the related corrosive conditions, where available, include the following:

- The production of methyl methacrylate and methacrylic acid—H₂SO₄ is used in this application. A zirconium unit built more than twenty years ago is still in service.
- The production of rayon by the viscose process—Although graphite equipment was initially used for the H₂SO₄-affected areas of the process, these have now been replaced with zirconium. Dramatic reductions in maintenance costs and downtime with the new equipment have improved operating efficiency and lowered overall energy costs.
- Glycolic acid is produced synthetically at high pressures (30 to 90 MPa) and temperatures (160 to 200°C). In this process, formaldehyde reacts with carbon monoxide and water in the presence of an acidic catalyst such as sulfuric acid, to form the acid. Zirconium is used in this process due to its well-known corrosion resistance in weak sulfuric acid at temperatures up to and above 260°C. It also has excellent erosion resistance.

For non-organic applications, zirconium is commonly used in the iron and steel industry to contain hot 5 to 40% H₂SO₄ used for pickling solutions. Care is required to ensure that the chloride ion concentration is very low because the presence of the high ferric ion content could cause ferric chloride pitting and corrosion. Zirconium is also used in H₂SO₄ recovery and recycle systems in which fluorides are not present, and the acid concentration does not exceed 65%.

II.5 HALIDE-CONTAINING PROCESSES

There are many process applications where zirconium is in contact with HCl. These include the production of concentrated HCl and polymers where zirconium has survived use as heat exchangers, pumps, and agitators for more than 15 years.

Since the 1970s, zirconium equipment has also provided excellent service in the synthetic production of lactic acid. The process is based on lactonitrile, which is produced by reaction of acetaldehyde and hydrogen cyanide at temperatures up to 200°C. The product is hydrolyzed in the presence of HCl to yield lactic acid. In areas where HCl is used, the selection of corrosion resistant materials is limited. Glass-lined materials, stainless alloys, and titanium and its alloys are unsuitable for a variety of reasons. Glass-lined materials are prone to breakdown, stainless alloys corrode and introduce toxic materials to the process stream, and titanium and its alloys are susceptible to crevice corrosion in hot chloride solutions. Fortunately, zirconium is ideal for the application provided; oxidizing HCl conditions resulting from the presence of ferric or cupric ions can be avoided. Zirconium is also highly resistant to crevice corrosion in chloride solutions.

Zirconium equipment is also used in the food industry for the breakdown of cellulose and in the polymerization of ethylene chloride, which is carried out in HCl and chlorinated solvents. The metal and its alloys are also strong contenders for an HI decomposer in hydrogen production. They resist attack by HI media (gas or liquid) from room temperature to 300°C compared to most stainless alloys, which only have adequate corrosion resistance at low temperatures.

II.6 NITRIC ACID-CONTAINING PROCESSES

Although stainless steel was originally the material of choice for most nitric acid production operations, process developments in the late 1970s found the limitations of this material; thus, it has since been superseded by zirconium.

Conventionally, HNO₃ is manufactured by oxidation of ammonia with air over platinum catalysts. The resulting nitrous oxide is oxidized to nitrogen dioxide and then absorbed in water to form HNO₃. Acid of up to 65% concentration is produced by this process although higher concentrations can be produced by dehydration.

Prior to the 1970s, a dual-pressure process was typically used in which the converter operated at about 500 kPa and the absorber at about 1100 kPa. The development of a mono-pressure process during the 1970s that operated at 1300 to 1500 kPa provided greater productivity, used smaller equipment, and permitted higher energy recovery capability. The first application of the mono-process in the late 1970s produced severe corrosion using 304L stainless steel components. Based on this experience, a series of corrosion tests were run on a range of stainless steels and zirconium alloys at a temperature of 204°C and acid concentrations up to 65%. From these tests it was clear that zirconium was the only suitable material for the mono-pressure process with corrosion rates consistently below 25 micron/year under the worst conditions. Subsequent use of zirconium in the production plant showed no sign of corrosion for almost 20 years in service.

As noted earlier, zirconium alloys are typically used in nuclear applications for cladding; however, they have also been used in SNF reprocessing plants where dissolution with nitric acid requires excellent corrosion resistance.

ATTACHMENT III

ZIRCONIUM-METALLURGY

III.1 GENERAL

Important phases in the history and development of zirconium and its alloys have been well documented by Etherington et al. (1955, pp. 1-5) and in ASTM STP 639 (1977, pp. 3-4) *Manual on Zirconium and Hafnium*. The following summarizes the data obtained from these and other sources.

Zirconium, as the element, was discovered in 1789, but the metal itself was not isolated until 1824 and then only in the form of a brittle, impure metal powder. It took a further hundred years to make a pure ductile metal through the development of the iodide decomposition process. Significant interest in the metal did not develop until the nuclear industry needed a material with relatively high strength, excellent high-temperature corrosion resistance, resistance to irradiation damage, and transparency to thermal neutrons. Since zirconium seemed to meet these requirements, efforts were devoted to the development of an economical production process. This was achieved in the late 1940s through the Kroll process. It later became evident that hafnium, which occurs naturally with zirconium, had a high neutron capture cross section. As a result of this observation, a process was developed to remove hafnium from the "commercial grade" zirconium.

Concurrent with process investigations on hafnium removal, a number of investigations focused on alloy development. Early test programs showed inconsistencies in the corrosion resistance of pure zirconium when exposed to high-temperature water and steam. Such abnormal behavior was attributed to the presence of minor impurities such as nitrogen and carbon (Kass 1964, pp. 5-6; Thomas 1955, p. 616). Alloy development programs were established in the early 1950s to mitigate these effects and to determine the effects of various elements on zirconium properties. Tin appeared to be the most beneficial alloying element. The composition, Zr-2.5% Sn, was initially chosen and designated Zircaloy-1. By 1952, it was shown that the corrosion rate of this alloy tended to accelerate with time; however, later research showed that this time-accelerated corrosion rate could be mitigated by a reduction in the tin content. The addition of small quantities of iron, nickel, and chromium to the alloy also provided beneficial corrosion resistance.

By 1965, zirconium alloys, particularly Zircaloy-2 and Zircaloy-4, were established in the U.S. as the predominant cladding material for boiling and pressurized water-cooled reactors (BWR and PWR), respectively. Other compositions, primarily those based on the zirconium-niobium alloy system, were under development and were subsequently used in the Canadian and the USSR nuclear programs.

III.2 ZIRCONIUM CHARACTERISTICS

Zirconium and its alloys are readily classified into two categories, nuclear and non-nuclear, as shown in [Table 6](#). All compositions have low alloy contents and are generally based on the low-temperature alpha structure with dilute additions of either solid solution strengthening or alpha stabilizing elements such as oxygen and tin. By contrast the niobium-containing alloys

may contain some niobium-rich beta particles, particularly those with higher niobium percentages.

The main difference between the nuclear and non-nuclear grades is the hafnium content. Nuclear grades have less than 100 ppm; whereas, the non-nuclear grades may contain up to 4.5% of the element. Although hafnium has a high neutron cross section and, therefore, a major impact on the nuclear properties of zirconium, its effect on the mechanical and chemical properties of zirconium and its alloys is minimal.

It is assumed from the above review that variations in the hafnium content have negligible impact on zirconium alloy corrosion rates, so that the corrosion data obtained on non-nuclear and nuclear grade materials are equivalent, and that the alloy composition of the non-nuclear grade Zr 704 (R60704) is sufficiently close to that of the nuclear grades Zircaloy-2 (R60802) and Zircaloy-4 (60804), that the corrosion characteristics of all three alloys can be considered comparable for similar processing conditions.

Table III.1 Nuclear and Non-nuclear Grades of Zirconium Alloys

Composition (wt%)										
Alloy design (UNS #)	Zr + Hf (min)	Hf (max)	Sn	Nb	Fe	Cr	Ni	Fe + Cr	Fe+Cr+ Ni	O (max)
Nuclear Grades										
Zircaloy-2 (R60802)	---	0.010	1.20-1.70	---	0.07-0.20	0.05-0.15	0.03-0.08	---	0.18-0.38	---
Zircaloy-4 (R60804)	---	0.010	1.20-1.70	---	0.18-0.24	0.07-0.13	---	0.28-0.37	---	---
Zr-2.5Nb (R60901)	---	0.010	---	2.40-2.80	---	---	---	---	---	---
Non-nuclear Grades										
Zr702 (R60702)	99.2	4.5	---	---	---	---	---	0.2 (max)	---	0.16
Zr704 (R60704)	97.5	4.5	1.0-2.0	---	---	---	---	0.2-0.4	---	0.18
Zr705 (R60705)	95.5	4.5	---	2.0-3.0	---	---	---	0.2 (max)	---	0.18

Regarding process conditions, most of the nuclear grade zirconium alloy material is processed into fuel cladding, guide tubes, and pressure tubes. Specific processes are used to guarantee material homogeneity (triple arc-melting minimum) and optimized microstructure (pilgering or rocking) for in-reactor cladding and guide tubes performance. This optimization provides a microstructure that orients the hydrides formed during corrosion into a circumferential direction. This orientation minimizes cladding failures from internal stresses. The pilgering process is also optimized to minimize cladding corrosion rates. Lesser quantities of nuclear grade zirconium alloys are processed into sheet material for use as spacer grids, water channels, and channel boxes. Such processes may not be optimized to the same extent as the cladding process because these components do not operate under such onerous corrosion conditions. Zircaloy bar is used for end-plug material.

Regarding non-nuclear applications, zirconium and its alloys are produced as ingots, forgings, pipes, tubes, plates, sheets, foils, bars, wires, and castings. These forms are used in the chemical processing industry (CPI) for heat exchangers, condensers, vaporizers, reactors, columns, piping systems, pumps, valves, and packing where excellent corrosion resistance is required. Details of CPI applications are given in Attachment II with specific attention to the corrosion resistance of zirconium and its alloys under adverse chemical conditions

III.3 GENERAL CORROSION OF ZIRCONIUM AND ITS ALLOYS

A general review of the corrosion resistance of zirconium and its alloys has been undertaken by Yau and Webster (1987, pp. 707-721). Although zirconium is a highly reactive element, as evidenced by its redox potential of -1.53 V versus the normal hydrogen electrode (NHE) at 25°C, it has a strong affinity for oxygen. In oxygen-containing media such as air, water, or

carbon dioxide, zirconium reacts at ambient temperature to form an adherent, protective surface-oxide film. This film is self-healing and protects the base metal from chemical and mechanical attack to temperatures of at least 350°C. As a result, zirconium is generally considered to be a highly corrosion-resistant metal. However, the protective oxide film does not readily form in a few media such as hydrofluoric acid, highly concentrated sulfuric acid, and certain dry organic halides. In addition, contact with ferric and cupric chloride has been shown to cause accelerated corrosion. Consequently, zirconium is not ideal for exposure in these media. Zirconium is also susceptible to localized corrosion such as pitting and SCC, when exposed to chloride solutions under oxidizing conditions. However, zirconium is not susceptible to crevice corrosion in chloride solutions since the condition in a crevice is normally reducing.

The report assumes that the evaluation can be restricted to those environments that are primarily to be anticipated in the spent nuclear fuel (SNF) repository. Although accelerated corrosion of zirconium and its alloys has been observed during contact with cupric chloride and organic halides, these conditions are not considered viable in the repository and are, therefore, not addressed in detail. It should also be stressed that there are significant differences between the condition of the spent nuclear fuel (SNF) cladding and the materials tested in the report. SNF cladding from PWRs is covered with zirconium oxide that typically varies between 5 and 100 microns in thickness while that from BWRs, although thinner, is still of the order of 5 to 20 micron. At these values the Zircaloy is oxidizing at a linear posttransition rate that is significantly slower than the pretransition rate observed in the early stages of Zircaloy oxidation. By contrast most of the non-nuclear corrosion results have been obtained on "clean" zirconium alloys with an oxide thickness significantly less than one micron. The observed and predicted corrosion rates obtained from these latter tests are expected to significantly overestimate the actual corrosion rates for SNF. Such overpredictions of the corrosion rates would also be expected from electrochemical tests typical of the types used in short-term experiments (hours/days). No specific references have been found regarding the use of chemicals to dissolve thick zirconium oxide films, but it is of interest to note that Bradhurst and Heuer (1970, p. 38) used a grinding technique to remove 2- to 50-micron oxides from samples during their oxide-stress experiments. This may imply that chemical dissolution of the oxide is a very slow process. Regarding the issue of zirconium oxide spallation, no specific studies have been found that quantitatively address the loss of oxide thickness. Spallation does not appear to occur below an initial oxide thickness of about 70 micron and, when spallation does occur, the loss is typically less than 30 micron. A minimum residual oxide of 40 micron thickness would therefore be expected on cladding when spallation occurs.

It is, thus, of some concern that the results and conclusions of this report may significantly overpredict corrosion rates since thin-film (pretransition) corrosion rates are generally much higher than thick-film (posttransition) rates.

III.4 ENVIRONMENTAL CONDITIONS—J-13 WELL WATER

Water used in nuclear reactors is very pure. It typically contains 20 to 50 ppm hydrogen in PWRs; whereas, in BWR systems the oxygen concentration is of the order of 200 ppb (Holzer and Stehle 1986, p. 26). By contrast, water used in the CPI, for example for cooling purposes,

may be severely contaminated. In both environments, zirconium and its alloys show excellent corrosion resistance when exposed to most types of water at temperatures well in excess of 100°C.

In principal, the repository conditions as represented by the J-13 well water would not be expected to produce any significantly different corrosion rates in zirconium and its alloys than those experienced in reactors. The well water analysis is given in Table III.2. The analysis shows a neutral solution with impurity concentrations too low to be corrosive to zirconium and its alloys. However, it has been hypothesized that ground water entering the repository may be concentrated in impurities as a result of evaporation. Table III.2 gives the predicted values. Of particular note is the fact that the halide content could become enriched due to the high solubility of most chlorides and fluorides. As a result, the corrosive potential of the water increases as the halide concentrations increase. However, the pH of the solution increases at the same time, and this is favorable because zirconium and its alloys are generally corrosion resistant at the higher pH values. That is, J-13 well water will not become oxidizing when the pH is so high. Conceivably, solution pH within crevices may become very acidic. As discussed in Section 6.1.10, the condition in a crevice would be too reducing to support the formation of oxidizing ions.

Since concentration of minerals can only occur concurrently with evaporation and coolant re-entry, fluoride corrosion and subsequent cladding failure would be predicted only if there is a breach in the waste package at this time. Thus any water that drips on the cladding will be a poorly defined salt solution but may be similar to the concentrated solutions shown in Table III.2 with the following modifications:

- A higher concentration of such dissolved metal ions as iron, nickel, chromium, etc.
- A more alkaline solution (higher pH value).

To simplify the discussion process, the greatly concentrated J-13 well water is divided into two cases, fluoride-free solution and fluoride-containing solution. The expected temperature is around 100°C, and the solution pH will be higher than 3.18.

Table III.2. Compositions of J-13 Well Water and Its Concentrates

Ion	Concentration (mg/liter)			
	J-13	Long Term Test Solution (1000X)	Beaker Evaporation (1000X)	90°C/ 85% Rel. Humidity
SO ₄	18.4	13000	15700	29500
Cl	7.14	7200	6120	14800
NO ₃	8.78	6440	6730	14200
F	2.18	1580	1520	3400
HCO ₃	128.9	47326	31471	11370
Na	45.8	42500	37700	77400
K	5.04	3580	3720	9700
Ca	13.0	3	7	25
Mg	2.01	1	0	0
SiO ₂ (aq)	61.0	109	7124	22500
pH	7.4	10.1	9.9	10

Note: Beaker Evaporation 1000X solution and Long Term Test 1000X solution agree reasonably well except the concentration of SiO₂ (aq). This disagreement could be attributed to the attack of the glass beaker by fluoride ions.